

Bacterial Translocation: Cause of activated intestinal macrophages in decompensated liver disease



by Johannie du Plessis

23362665

Dissertation submitted in partial fulfilment of the degree of
Master of Science
in the Department of Immunology, Faculty of Health Sciences,
University of Pretoria, Pretoria, South Africa
Supervisor: Prof Schalk W van der Merwe

Date: September 2011

Abstract

Background and Aim: Bacterial infections are a well described complication of cirrhosis and occur in 37% of hospitalized patients. Culture positive infections in addition to the presence of bacterial products and DNA lead to loss of liver function and decompensation in cirrhosis. The mechanisms and molecular pathways associated with Bacterial Translocation (BT) are unknown. The aims of this study were to determine: i. macrophage phenotype and molecular pathways associated with bacterial translocation ii. if intestinal macrophages in liver cirrhosis are capable of modulating intestinal permeability.iii. structural integrity of the epithelial barrier.

Methods: Duodenal biopsies and serum samples were collected from 29 patients with decompensated cirrhosis, 15 patients with compensated and 19 controls. Duodenal macrophages were characterized by means of flow cytometry and IHC. Gene expression analysis was performed to determine molecular pathways involved in BT. Inflammatory cytokine determination was done in serum and culture supernatant by means of customized cytometric bead arrays.

Results: Patients with decompensated cirrhosis demonstrated: increased frequency of CD33+/CD14+/TREM-1+ and iNOS+ macrophages in their duodenum, elevated mRNA levels of nitric oxide synthase 2 (NOS2), chemokine ligand 2 (CCL2), chemokine ligand 13 (CCL13) and interleukin 8 (IL8) and increased serum levels of interleukin 6 (IL6), IL8 and lipopolysaccharides (LPS). Additionally, patients with decompensated cirrhosis showed an increase in NO, IL6, IL8 and CCL2 levels in culture supernatant after short term duodenal biopsy culture. Although the epithelial barrier on EM seemed intact, significantly increased expression of the “pore” forming tight junction claudin 2 was observed.

Conclusion: This study showed the presence of activated CD14⁺Trem-1⁺iNOS⁺ intestinal macrophages and increased levels of NO, IL-6 and claudin-2 levels in the duodenum of patients with decompensated liver cirrhosis, suggesting that these factors enhance intestinal permeability to bacterial products.

Keywords: Liver cirrhosis, decompensated cirrhosis, bacterial translocation, intestinal macrophage, intestinal epithelial barrier, tight junctions, activation, iNOS, IL6, IL8, CCL2, claudin 2

Samevatting

Inleiding: Bakteriële infeksie is 'n beskryfde komplikasie van lewersirroze wat in 37% van gehospitaliseerde pasiente voorkom. Kultuur positiewe infeksies asook die teenwoordigheid van bakteriële produkte en DNA lei tot verlies van lewerfunksie en dekompensasie. Die molekulere meganismes wat verband hou met bakteriële translokasie is nog onbekend. Die doel van hierdie studie was om: i. Makrofaag fenotipe en molekulere meganismes geassosieer met bakteriële translokasie te beskryf, ii. te bepaal of intestinale makrofage dermdeurlaatbaarheid beïnvloed, asook iii. om die strukturele integriteit van die dermwand te bepaal.

Methods: Serum en dunderm biopsies was verkry van 29 pasiente met gedekompenseerde lewer sirrose, 15 pasiente met gekompenseerde sirrose en 19 kontroles. Dunderm makrofage was gekarakteriseer met behulp van vloesitometrie en immunohistochemie. Molekulere meganismes belangrik tydens bakteriële translokasie was bepaal met behulp van genekspressie. Serum en selkultuur supernatant sitokien bepaling was met Bioplex assays gedoen.

Resultate: Pasiente met gedekompenseerde sirrose demonstree: 'n verhoogde frekwensie van CD33+/CD14+/TREM-1+ en iNOS+ makrofage in hul dunderm, verhoogde mRNA vlakke van NOS2, CCL2, CCL13 en IL8 asook verhoogde serum vlakke van IL6, IL8, LPS. Addisioneel het pasiente met gedekompenseerde sirrose verhoogde supernatant vlakke van NO, IL6, IL8 and CCL2 na kort termyn dunderm biopsie kulture. Alhoewel elekronmikroskopie gewys het dat die dundermwand intak is, was daar statisties-beduidend verhoogde ekspressie van die "porie" vormende vaste-aansluitings-proteïen, claudin 2 sigbaar.

Gevolgtrekking: Gesamentlik het die studie gewys dat geaktiveerde CD14⁺/Trem-1⁺/iNOS⁺ intestinale makrofage asook verhoogde vlakke van NO, IL-6 en claudin-2 teenwoordig is in die dunderm van pasiente met gedekompenseerde sirrose. Dit dui daarop dat dië faktore dermdeurlaatbaarheid vir bakteriële produkte kan verhoog.

Table of contents

CONTENTS	Page
Title Page	ii
Abstract	iii
Samevatting	iv
List of Tables	v
List of Figures	v
Abbreviations	vi
 CHAPTER ONE	
Introduction and Aims	1
 CHAPTER TWO	
Materials and Methods	4
 CHAPTER THREE	
Results	13
 CHAPTER FOUR	
Discussion	27
 CHAPTER FIVE	
Summary	32
 REFERENCES	34
 APPENDICES	
Appendix A	
Flow cytometry histograms	38
Appendix B	
Nanodrop and Experion readings	42
Appendix C	
Amplification and Melt curves	43
Appendix D	
Genes included in the Human Inflammatory response and Autoimmunity (PAHS-077A) RT ² Profiler TM Array	44

Appendix E		
	Genes included in CAPH09859D customized RT ² Profiler PCR array	48
Appendix F	Ethics Approval	50
DECLARATION		51
ACKNOWLEDGEMENTS		52

List of Tables

	Page
Table 1	
Number of samples included in each experimental investigation	12
Table 2	
Clinical characteristics of Patients included in the study	13
Table 3	
Genes of significance in decompensated cirrhosis	20

List of Figures

	Page
Figure 1	
Summary of experimental procedures	4
Figure 2	
LPS plasma levels in different patient groups and CD33+/CD14+/TREM-1+ macrophage frequency	14
Figure 3	
CD68 histology results	16

Figure 4		
	iNOS histology results	18
Figure 5		
	Results for plasma cytokine levels in each patient group, as well as total nitrite and cytokine analysis in culture supernatant	21
Figure 6		
	TEM pictures	24
Figure 7		
	Results of tight junction protein determination including densitometry analysis	24
Figure 8		
	Summary- normal intestine	32
Figure 9		
	Summary- decompensated intestine	33

Abbreviations

APC: allophycocyanin

ASH: alcoholic steatohepatitis

BT: bacterial translocation

BSA: bovine serum albumin

bactDNA: bacterial DNA

CCL2/MCP-1: chemokine (C-C motif) ligand 2

CCL13: chemokine (C-C motif) ligand 13

CRP: C-reactive protein

DAB: diaminobezidine

CD3: cluster of differentiation 3

CD14: cluster of differentiation 14

CD16: cluster of differentiation 16

CD19: cluster of differentiation 19

CD68: cluster of differentiation 68

CD80: cluster of differentiation 80

CD86: cluster of differentiation 86

EDTA: ethylenediaminetetraacetic acid

FITC: fluorescein isothiocyanate

GAPDH: glyceraldehyde-3-phosphate dehydrogenase

HPF: high power fields

IEC: intestinal epithelial cells

IL6: interleukin 6

IL8: interleukin 8

IL10: interleukin 10

INR: international normalized ratio

iNOS/NOS2: nitric oxide synthase 2, inducible

IBD: inflammatory bowel disease

LAL: limulus amoebocyte lysate

LM: light microscopy

LPS: lipopolysaccharides

MMC: mononuclear cells:

PHT: portal hypertension

PVDF membrane: Polyvinylidene fluoride membrane

PBS: phosphate buffered saline

PEB: phosphate buffered saline with 0.5% bovine serum albumin

PE: phycoerythrin

SBP: spontaneous bacterial peritonitis

SIRS: systemic inflammatory response syndrome

SDS-PAGE: sodium dodecyl sulfate polyacrylamide gel electrophoresis

SD: standard deviation

TBS: tris buffered saline

TEM: trans electron microscopy

TREM-1: triggering receptor expressed on myeloid cells 1

TLR-2: toll-like receptor 2

TLR-4: toll-like receptor 4

TJ: tight junction

TNF- α : tumor necrosis factor alpha

NASH: non-alcoholic steatohepatitis

NEC: necrotizing enterocolitis

NO: nitric oxide

Chapter One: Introduction and Aims

Cirrhosis is a progressive disease with potentially fatal complications. Once decompensation has occurred in all types of liver disease, mortality without transplantation is as high as 85% over 5 years ¹.

Bacterial infection is a common complication that occurs in advanced liver cirrhosis ². Infections frequently accelerate decompensation of underlying liver disease and are consequently associated with a considerably higher morbidity and mortality ^{3,4}. Recent data suggest that between 15%-35% of cirrhotic patients admitted to hospital developed nosocomial bacterial infection, substantially higher compared to 5-7% in the general hospital population ⁵.

Higher endotoxin concentrations are found in the peripheral blood of cirrhotics than in healthy subjects with a statistically significant gradient between portal and peripheral blood, highlighting the role of the bowel as the source of endotoxin ⁶.

Bacterial translocation (BT), which is defined as the movement of viable microbes and microbial products from the intestinal lumen to extra intestinal sites, is considered a key event in the pathogenesis of bacterial infections in cirrhosis ⁷.

In human cirrhosis the incidence of BT is also related to the degree of portal hypertension (PHT) and liver dysfunction reported in approximately 30-40% of cirrhotics with ascites and more frequently in Child C than Child A and B cirrhosis ⁶. It has recently been shown that not just viable bacteria but also bacterial DNA (BactDNA) translocation is a frequent and important event in patients with cirrhosis and ascites without culture positive infections. It is also associated with a significant inflammatory reaction similar to that observed in patients with spontaneous bacterial peritonitis (SBP) ^{8, 9, 10}.

Although BT is a well described event in cirrhosis, a clear etiopathogenic mechanism behind the origin of BT is still lacking. The presence of small intestinal bacterial overgrowth, hyperdynamic portal status and impairment of the intestinal barrier has been purposed as causes of this phenomenon ¹¹.

The intestinal wall constitutes the largest and one of the most important physical barriers against the external environment and BT¹². The intestinal surface is lined by a single layer of columnar intestinal epithelial cells (IEC) that acts as a selectively permeable barrier, permitting the absorption of nutrients, electrolytes and water while maintaining an effective defence against intraluminal toxins, antigens and intestinal flora¹³. Specialized cell-cell junctional complexes allow for selective paracellular permeability (tight junctions (TJ)), maintain intra cellular adhesion (intermediate junctions and desmosomes) and permit intracellular communication (gap junctions)¹⁴.

The intestinal barrier is complex in the fact that it not only performs essential barrier functions, obstructing the entry of commensal and pathogenic organisms but is also necessary to regulate and maintain immune homeostasis. If it fails to perform either one of the above functions the balance between tolerance and immunity can contribute to the pathogenesis of numerous inflammatory conditions including, inflammatory bowel disease (IBD), necrotizing enterocolitis, food allergies and cancer¹⁵.

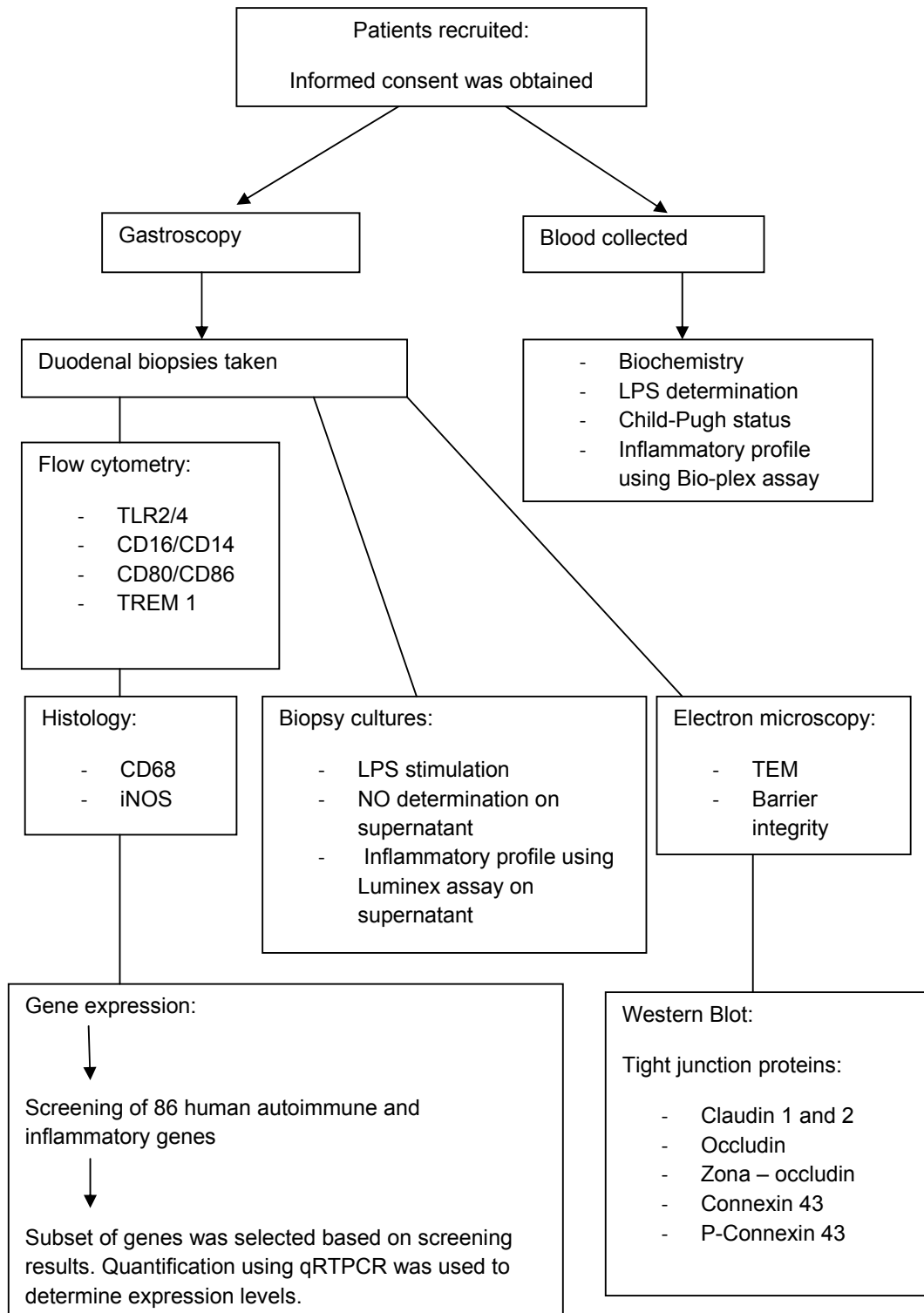
Macrophages in the intestinal tract represent the largest pool of tissue macrophages in the body¹⁶. Macrophages form part of the innate immune system that regulate inflammatory responses to bacteria, protect the mucosa from harmful pathogens and scavenge dead cells and foreign debris¹⁶. Intestinal macrophages are distinctly different in phenotype and function compared to blood monocytes¹⁷. Innate immune receptors such as CD14 and TREM-1, as well as growth receptors (CD25, CD123) are not expressed by intestinal macrophages. They also do not produce inflammatory cytokines in response to an array of inflammatory stimuli but retain avid phagocytotic and bactericidal activity^{16, 17}. This profound inflammatory anergy displayed by intestinal macrophages give them the ability to maintain intestinal homeostasis by protecting the host from foreign pathogens and negatively regulating excess immune response to commensals¹⁸.

The aim of this study was to gain a better understanding of the mechanism of BT by investigating some of the principal factors that normally prevent it, such as **epithelial barrier integrity** specifically the **intestinal tight junctions**. Additionally immunocompetence with special focus on **intestinal macrophage phenotype, nitric oxide (NO)** production and

inflammatory pathways associated with decompensated and compensated liver cirrhosis were also assed.

Chapter Two: Materials and Methods

Figure 1. Summary of Experimental Procedures



Study population and setting

Patients with liver cirrhosis referred to the Interventional endoscopy unit, Pretoria East hospital for the evaluation of liver disease and the management of portal hypertension from January 2008 to February 2011, were considered for this investigation. In all patients cirrhosis was diagnosed by a combination of standard clinical, biological, ultra sonographical, and/ or histological criteria. Patients were included or excluded from the study based on the following criteria:

Inclusion criteria:

- Age between 18 and 80 years
- Confirmed diagnosis of NASH or alcoholic liver cirrhosis

Exclusion criteria:

- Any other cause of liver cirrhosis other than NASH or alcoholic liver disease
- Severe sepsis or SIRS with evidence of circulatory dysfunction or requiring inotropic support
- Hepatocellular carcinoma
- Portal vein thrombosis
- Cardiac, renal or respiratory failure
- Previous luminal gastrointestinal surgery
- Bacterial infection or treatment with antibiotics in the preceding 6 weeks
- Alcohol use in the preceding 6 weeks

The selected patient population was further subdivided into the following groups:

Group 1: Decompensated cirrhosis - Patients with cirrhosis presenting with new onset ascites with or without variceal bleeding encephalopathy or jaundice (N=29).

Group 2: Compensated/uncomplicated cirrhosis - Patients with confirmed cirrhosis without ascites, encephalopathy, or a history of variceal bleeding or a previous episode of decompensation (N= 15).

Control group: Patients without any chronic liver disease undergoing endoscopy for reflux disease or dyspepsia symptoms (N=19).

The protocol was approved by the University of Pretoria, Ethics Committee and followed the principles of the Declaration of Helsinki. Written informed consent to participate in the study was obtained from each patient.

Sample collection

Tissue samples

Patients included in the study underwent upper gastrointestinal endoscopy for variceal screening. During endoscopy all findings were recorded including esophageal and gastric varices, size of varices as well as signs of portal hypertensive gastropathy. In stable patients not actively bleeding a total of “10-12” duodenal pinch biopsies were obtained from the third part of the duodenum at endoscopy using a Radial III biopsy forceps (Boston Scientific). Biopsies for flow cytometry were placed on ice in RPMI 1640 and processed within 4 h. Biopsies for histology were fixed immediately in either 10% formalin for light microscopy (LM) or 2.5% glutaraldehyde-formaldehyde for transmission electron microscopy (TEM). Biopsies for gene expression analyses and western blot were snap frozen and stored at -80°C. In a subgroup of patients biopsies were placed in cold, sterile PBS for short-term culture studies.

Biochemistry

In all patients blood samples were collected from a peripheral vein into sterile tubes, centrifuged, and process immediately for biochemical analysis which included standard full blood count, liver function tests, INR, CRP. Additional blood samples were obtained centrifuged and stored at -80°C for LPS and plasma cytokine evaluations. All samples were processed under sterile conditions and in airflow chambers.

Plasma LPS levels

Circulating endotoxin levels were quantified using the Limulus Amoebocyte Lysate (LAL) assay QCL-1000 (Lonza, Valais Switzerland). Plasma

samples were diluted 1:3 with LAL Reagent Water, inactivated (30 min, 65°C) and analysed in duplicate in 96 well plates.

Plasma Cytokine determination

Cytokine and chemokine levels in plasma were quantified using customized Bio-PlexPro™ (Bio-Rad, Hercules, CA) assays. The following cytokines were assessed: IL-8, CCL2/MCP-1, IL10, IL-6 and TNF α . Assays were performed according to manufacturer's protocol. Plasma samples were diluted 1:4 with sample diluent and were tested in duplicate in 96 well plates.

Isolation of mucosal mononuclear cells (MMCs)

A single-cell suspension from duodenal biopsies was obtained by means of GentleMACSdissociator (MiltenyiBiotec, Gladbach Germany) according to manufacturer's instructions. In short, duodenal biopsies were digested in RPMI 1640 containing 1.0 mg/ml collagenase type IV (Sigma, St. Louis, MO) (37°C for 30 min.)The single cell suspension was then passed through a 70- μ m cell strainer (Becton Dickenson Labware, NJ) and washed with sterile PBS with 0.5% BSA (PEB buffer) (MiltenyiBiotec, Gladbach Germany) to remove debris.

Determination of macrophage phenotype

Biopsy single cell preparations in PEB buffer were stained with 20 μ l monoclonal antibodies (Mabs)/ 100 μ l of 10^6 cells, incubated for 20 min at room temperature in the dark. The Mabs were used in two-colour combinations as follows: CD14-PE-Cy7 (eBioscience, San Diego, California, USA) with CD33-APC (Siglec-3, R&D Systems,Minneapolis, USA)); CD16-FITC (Beckman Coulter, Miami, FL, USA) with TREM-1-PE (R&D Systems,Minneapolis, USA)); CD80 (B7-1)-FITC, (R&D Systems,Minneapolis, USA)) with CD86 (B7-2)-PE (eBioscience, San Diego, California, USA); TLR-2-FITC (TL2.1, eBioscience, California, USA) with TLR-4-PE-Cy7 (HTA125, eBioscience, San Diego, USA). Samples were processed for analysis in the Beckman Coulter TQ-Prep system,

which lysis any remaining contaminating erythrocytes and fixes the Mabs to the cell surface. For accurate counting, 100 μ l of Flow-Count™ Fluorospheres (Beckman Coulter, Miami, FL, USA), was added. Cells were then analysed by flow cytometry on the Beckman Coulter Cytomics FC500 cytometer fitted with a 488nm blue laser and a 635nm solid-state red laser, using 2-colour protocols and the CXP Software (Beckman Coulter, Miami, FL, USA) (see appendix A).

The macrophage population within the total cell population was identified using orthogonal light scatter features, together with CD14, CD 33 and CD16 expression.

To assess and confirm the purity of the prepared biopsy specimen, the cells were, in addition, incubated with CD3-FITC and CD19-PE (Beckman Coulter, Miami, FL, USA), to identify the lymphocyte population, which was used as the internal reference population within the total cell population assessed (see appendix A).

Gene expression

Total RNA was extracted from duodenal biopsies using the RNeasy kit in combination with RNase-Free DNase (Qiagen, Hilden, Germany). The quantity and quality of the RNA was confirmed by Nanodrop ND1000 (Thermo Scientific, DE, USA) and Experion™ system (Bio-Rad, Hercules, CA) analysis respectively. cDNA was synthesized from 2.0 μ g of total RNA using the RT² PCR array first strand kit (SABioscience, Frederick, MD). The expression levels of 84 general inflammatory genes using the human Inflammatory response and Autoimmunity RT² Profiler PCR array (see supplemental text) (SABioscience, Frederick, MD) were assessed by semi-quantitative RT-PCR in 96 well plates using RT² SYBR Green qPCR Master Mix and a CFX96 Real Time PCR Detection System (BioRad, Hercules, CA) platform. Fifteen decompensated cirrhotics and 5 controls were analysed. Data was normalized using five different housekeeping genes and analyzed by the comparative cycle threshold method using REST 2009 V2.0.13 software (Qiagen, Hilden, Germany).

Genes that were up regulated during the screening as well as alternative inflammatory pathways that were not included in the screening assay in

combination with the two most stable housekeeping genes as determined by geNorm software were included in a custom expression assay.

In the customized expression assay the levels of 27 genes associated with inflammation were determined using the human CAPH09859D customized RT² Profiler PCR array (SABioscience, Frederick, MD) (See supplemental text). Fourteen decompensated cirrhotic, seven compensated cirrhotic and six controls were analysed in triplicate. Data was normalized using two housekeeping genes and analysed by the comparative cycle threshold method using REST 2009 V2.0.13 software (Qiagen, Hilden, Germany).

Duodenal Biopsy cultures

Culture supernatants of intestinal biopsy samples for detection of NO and local cytokine production were prepared as described^{19, 20}. Biopsy samples were immediately placed in phosphate buffered saline extensively washed (five times). All biopsy samples were weighed and incubated in 1ml RPMI 1640 medium containing 10% fetal calf serum (Sigma), 10µl/ml Pen/Strep Amphotericin B (Cambrex, Walkersville, MD) and 1µl/ml gentamicin (Genta 50, PhenixPharmaceuticals, Belgium) at 37°C in a humidified 5% carbondioxide/95% air atmosphere for 48 hours. One biopsy sample was incubated with Lipopolysaccharide (LPS) (1ug/mL, Sigma) and another without LPS. Supernatants were stored at -80°C until further analysis.

Nitric oxide determination in culture supernatant

Total nitrite and nitrate in supernatant were determined by Total Nitric Oxide and Nitrite/Nitrate Assay (R&D Systems, Minneapolis, USA) according to manufacturer's protocol. Supernatant samples were centrifuged to remove particles, diluted 1:5 with reaction diluent and tested in triplicate in 96-well plates.

Supernatant Cytokine determination

Cytokine and chemokine levels in culture supernatant were quantified using customized Bio-PlexPro™ (Bio-Rad, Hercules, CA) assays. The following cytokines were assessed: IL-8, CCL2/MCP-1, IL10, IL-6 and TNF α . Assays were performed according to manufacturer's protocol. Plasma samples were tested in duplicate in 96 well plates.

Histological and ultra-structural analysis of the duodenal wall

Histological analysis was conducted by an experienced gastrointestinal pathologist blinded to the subgroups. Routine light microscopy was carried out on haematoxylin and eosin-stained 3 μ m sections of biopsy tissue processed to paraffin wax. CD68 immunoperoxidase was performed on tissue sections which had undergone heat retrieval in a PT101 Link Pre-Treatment Module (Dako, Denmark). Following blocking of endogenous peroxidase, tissue sections were incubated with FLEX mouse anti-human CD68 clone KP1 (Dako, Denmark), treated with Envision™/HRP dual link polymer, visualized with diaminobenzidine (DAB) chromogen and counter-stained with haematoxylin. The number of CD68⁺ cells in five representative high power fields (HPF) of 0.80 mm² (magnification x 400) was counted and the results reported as the average number of macrophages/HPF. iNOS staining was performed on sections after heat mediated retrieval in PT101 Link Pre-Treatment Module at pH = 9. After blocking of endogenous peroxidase, sections were incubated with a dilution of rabbit polyclonal to iNOS (Abcam, Cambridge, UK), treated with Envision™/HRP dual link polymer, visualized with DAB and counter-stained with haematoxylin. The number of macrophages demonstrating cytoplasmic staining was counted in five representative high power fields (magnification x 400) and reported as the average number of cells/HPF. Glutaraldehyde-fixed specimens were placed in 1% osmium tetroxide and embedded in quetol resin for Transmission Electron Microscopy (TEM). TEM sections were contrasted with uranyl acetate and lead citrate and analyzed on a JOEL JEM 2100F microscope. TEM analysis was done by the Department of Anatomy University of Pretoria.

Western blot protein analysis

Western blot analysis was performed from membrane extracts of duodenal biopsy specimens. Biopsies were individually weighed and lysed in sample buffer containing 50 μ M Tris-HCL, pH7.4, 100 μ M NaCl (Merck, New Jersey, USA), 10 μ M EDTA, 50 μ M NaF, 500 μ M Na₃VO₄, 1% Triton X-100, 1Nm PMSF (Sigma Chemical Co., St Louis, MO) and 1X Protease inhibitor cocktail (Roche, Basel, Switzerland). For the extraction of non soluble proteins biopsies were lysed in sample buffer containing 50mM Tris-HCl, 50mM NaCl, 1mM DTT, 0.5% Tween-20, 1% N-larkosylsarkosine, 1% SDS, 1% Triton X-100 (Sigma Chemical Co., St Louis, MO) and 1X Protease inhibitor cocktail (Roche, Basel, Switzerland). The samples were then sonicated with a Sonifier cell disruptor B-30 (Branson Sonic Power Co., Danbury, CT, USA) at 20% duty cycle and output control of 4, for 10sec. Protein concentrations were determined by using the Bio-Rad protein assay kit with Bovine Serum Albumin as a standard (Bio-Rad, Hercules, CA). Sample aliquots of 75 μ g were separated by SDS-PAGE using the Laemmli method. Proteins, Claudins, Connexin 43, Connexin 43(pS368), Occludin were separated on 12% gels while the Zona-occludins were separated on 7% gels. Proteins were transferred to polyscreenpolyvinylidenedifluoride (PVDF) transfer membrane (Bio-Rad) using a Hoefer SE300 blotting cell (Amersham, UK) according to manufacturers instruction. Membranes were then incubated in Protein-free blocking reagent (Thermo Scientific, Waltham, MA) for 1h at room temp, washed with PBS/0.1% Tween-20 and further incubated with primary antibody for each tight junction protein (Claudin I, Claudin II, Connexin-43, Occludin and Zona-Occludin) respectively. Alkaline phosphatase conjugated secondary antibody was used in conjunction with the Bio-Rad AP detection kit (Bio-Rad, Hercules, CA) to detected bound antibodies. Primary antibodies against tight junction proteins were provided by Invitrogen (Camarillo, CA) while antibodies for reference proteins GAPDH and β -actin were provided by Serotec (Kidlington, Oxford, United Kingdom). The use of antibodies and detection of proteins was done according to the manufactures instruction. Densitometric comparisons were carried out on

the blots using the Quantity One 1D analysis software from the Bio-Rad discovery series.

Statistical analysis

All data was entered into a Microsoft Excel 2007 spreadsheet. Using Statistix 9 (Analytical software, Tallahassee, FL, USA) non parametric comparisons between observations in different groups were conducted with the Wilcoxon Rank Sum test. Comparisons between paired observations within groups was done with the Wilcoxon Signed Rank test. Two proportion Fischer exact tests were used for binary variables. Two-tailed p-values ≤ 0.05 were considered significant. Where appropriate, linear correlations were assessed using Spearman's rank correlation coefficient.

Table 1: Summary of samples and patients numbers included for each investigation

Investigation	Decompensated	Compensated	Control
Total sample number included	n=29	n=15	n=19
Plasma LPS determination	n=25	n=14	n=19
Plasma cytokines analysis	n=16	n=13	n=17
Flowcytometry	n=12	n=10	n=12
Gene Expression analysis	n=14	n=7	n=6
Histology – CD68	n=21	n=11	n=7
Histology - iNOS	n=13	n=11	n=11
Westernblot – ZO-1	n=4	n=4	n=3
Westernblot - Rest	n=10	n=4	n=6
Biopsy cultures	n=10	n=5	n=7
Supernatant cytokine analysis	n=7	n=4	n=5
Supernatant- total nitrite	n=7	n=4	n=6

Chapter Three: Results

Clinical Data

Clinical characteristics of the enrolled population are summarized in **Table 2**. No significant difference with regard to age and gender were observed among groups. As expected, all the clinical markers such as low albumin, increased INR and bilirubin that are associated with advanced liver disease were significantly elevated in decompensated cirrhosis compared to compensated cirrhosis and healthy controls.

Table 2. Clinical characteristics of Patients included in the study

Variable	Decompensated (n= 29)	Compensated (n=15)	Control (n=19)
Age (yr)	60 ±10	57 ±10	63 ±10
Gender, male %	62%	40%	37%
Etiology of Liver disease			
Alcoholic	19	3	0
NASH	10	12	0
Child-Turcotte-Pugh score (points)	9.1 (7-11)	5.5 (5-7)	5
Child-Turcotte-Pugh score (A/B/C)	(0/14/15)	(13/2/0)	0
Serum albumin (g/L)	2.8 ± 0.44*†	3.6 ± 0.57†	3.5 ± 0.28*
INR	1.6 ± 0.42*†	1.1 ± 0.08†	1.1 ± 0.22*
Serum bilirubin (mg/dL)	5.19 ± 3.47*†	0.99 ± 0.41†	0.78 ± 0.38*
Platelets (10 ⁹ /L)	103.74 ± 55.04*†	156.33 ± 69.56*†	277.06 ± 83.29*•
White cell count (10 ⁹ /L)	7.13 ± 4.45	4.63 ± 2.23	6.08 ± 2.30
Positive Blood culture (n(%))	3(10%)	0	0
Ascites (n (%))	22(76%)	0	0
Variceal Bleeding (n (%))	3 (10%)	0	0
Encephalopathy (n(%))	8 (28%)	0	0
Esophageal varices, n(Small/Large)	25 (10/15)	7 (4/3)	0

Notes: Child-Turcotte-Pugh score is represented as mean and range.

Other results are expressed as mean ± SD.

Abbreviations: INR: international normalized ratio, SD: standard deviation

*P< 0.05: Decompensated patients versus Controls

•P<0.05: Compensated patients versus Controls

†P<0.05: Decompensated patients versus Compensated

LPS levels are significantly elevated in the plasma of decompensated patients and correlate with Child-Pugh status

Significantly increased plasma LPS levels were observed in decompensated liver cirrhosis (0.916 ± 0.438) versus healthy controls (0.712 ± 0.182) ($p = 0.03$) (**Figure 2A**). No increases in LPS levels in the serum of compensated liver cirrhosis (0.797 ± 0.355) compared to controls (0.712 ± 0.182) were present. A weak but significant correlation was found between Child-Pugh score and LPS ($r = 0.292$, $p = 0.03$).

CD14 and TREM1 expressing macrophages are significantly increased in the duodenal mucosa of decompensated patients

As previously shown, intestinal macrophages generally display a specific phenotype that lack the LPS receptor, CD14 but still retain potent phagocytotic and bacteriocidal activity¹⁷. To describe the intestinal macrophage phenotype in patients with decompensated liver cirrhosis we screened duodenal biopsies using flowcytometric analysis. The number of intestinal macrophages that expressed the LPS receptor (CD14) was significantly increased in the intestine of patients with decompensated liver cirrhosis (**figure 2B**). These CD33+/CD14+ macrophages also co-expressed other activation markers such as TREM-1, which was significantly elevated in the small intestine of decompensated liver disease (42.58 ± 15.20) versus controls (22.86 ± 10.81) ($p = 0.01$) (**figure 2C**).

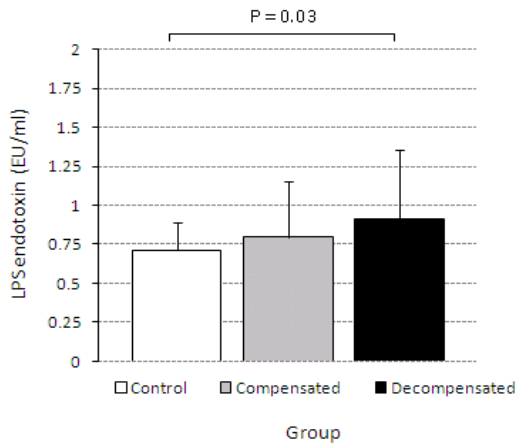
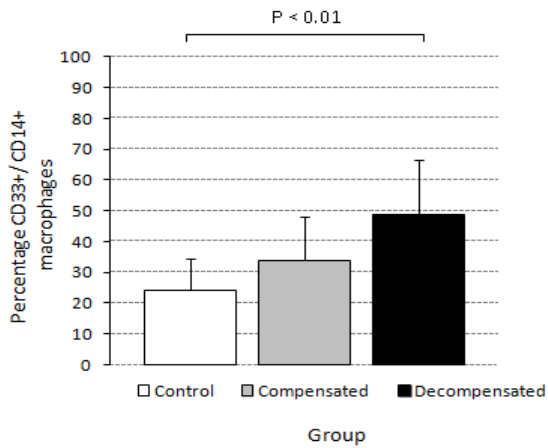
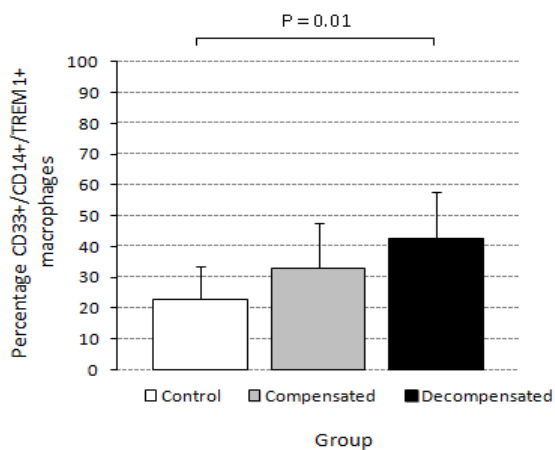
A

B

C


Figure 2. Patients with decompensated liver disease had significantly higher levels of LPS in their serum compared to controls (A). The frequency of CD14 expressing macrophages were significantly increased in the small

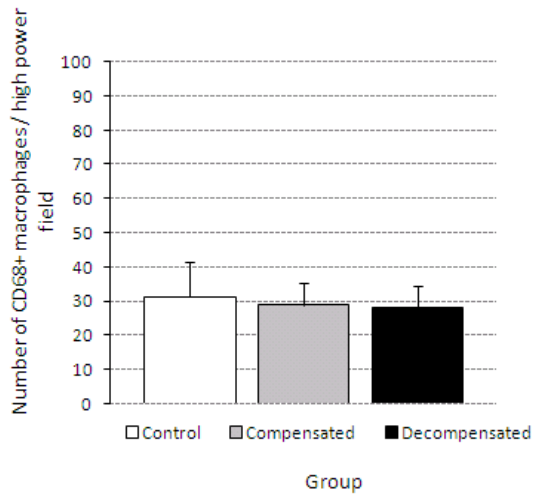
intestine of patients with decompensated liver disease (B). Not only do these macrophages express higher numbers of CD14, they also co-express other activation markers such as TREM-1 at a significantly higher frequency (C).

Intestinal macrophages show similar CD68⁺ expression and distribution but increased iNOS synthesis by immunohistochemistry

To further characterize the macrophage population in the small intestine of decompensated liver cirrhosis, we looked at the amount and distribution of intestinal macrophages by means of IHC. CD68 was used as marker for all monocytes and macrophages. iNOS typically produced by activated macrophages was used to determine if these macrophages were activated.

Immunohistochemical staining showed comparable numbers of CD68⁺ macrophages in decompensated, compensated and control subjects: decompensated cirrhosis vs. controls (28.14 ± 6.40 vs. 31.21 ± 10.41 ; CD68⁺ macrophages/mm²) and compensated vs. controls (28.82 ± 6.43 vs. 31.21 ± 10.41 ; CD68⁺ macrophages/mm²) (**figure 3 A-D**). However, there was a significant increase in the number of cells that stained positive for iNOS in both decompensated cirrhosis compared to controls (91.25 ± 14.44 vs. 54 ± 9.82 macrophages/mm²) ($p < 0.01$) and never decompensated cirrhosis compared to controls (83.24 ± 12.68 vs. 54 ± 9.82 macrophages/mm²) ($p < 0.01$) (**figure 4 A-D**).

A



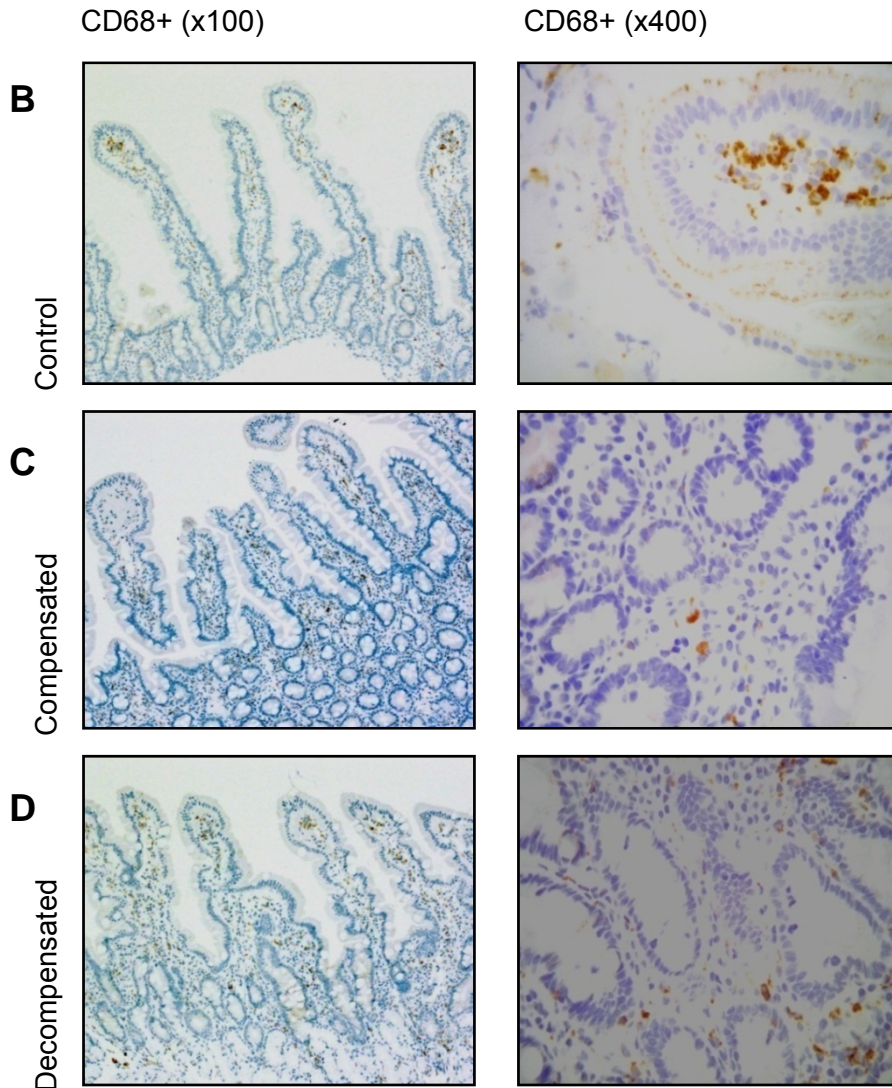
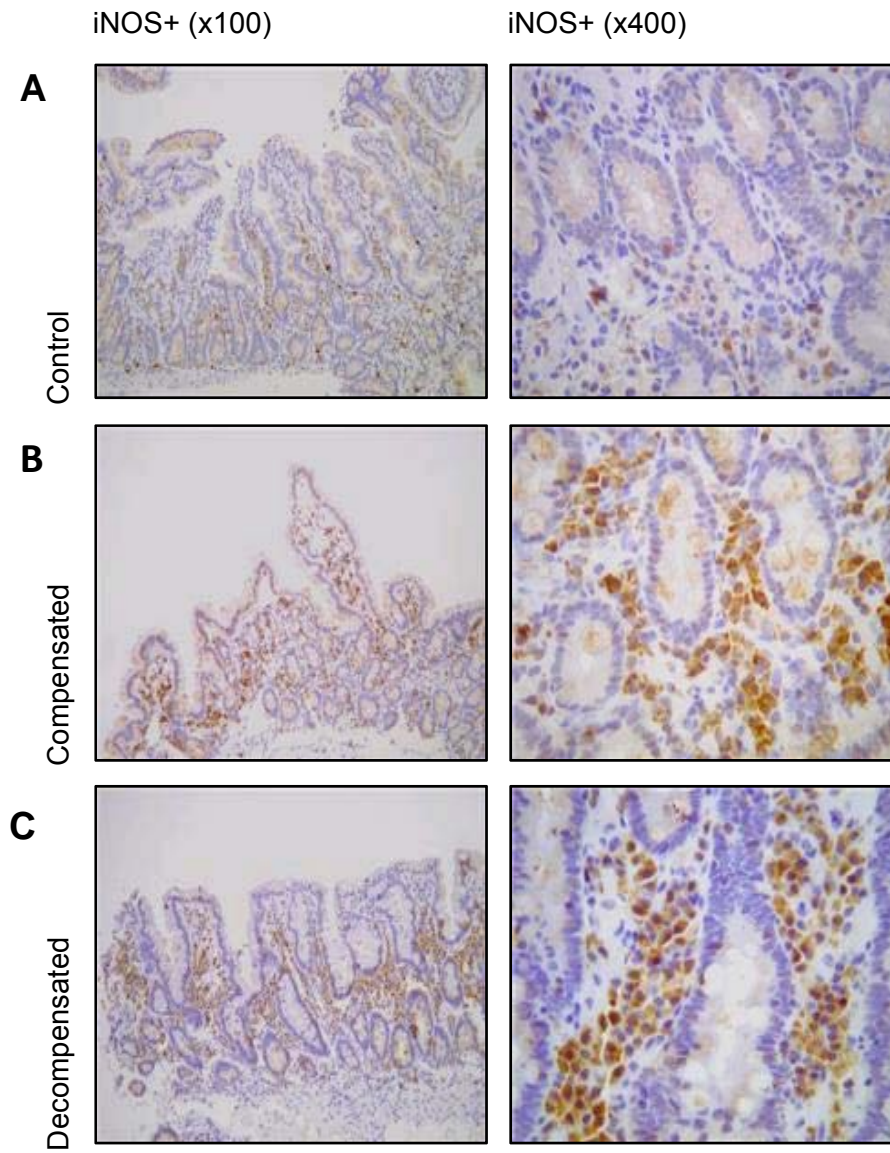


Figure 3. The number and distribution of CD68 positive macrophages did not differ between the groups (A). The presence of CD 68 positive macrophages was assessed by immunohistochemistry on paraffin-embedded tissue collected at endoscopy in controls, compensated and decompensated liver cirrhosis. Representative microphotographs are shown at low (x100) and high power (x400) magnification of controls (B), compensated cirrhosis (C) and decompensated cirrhosis (D).



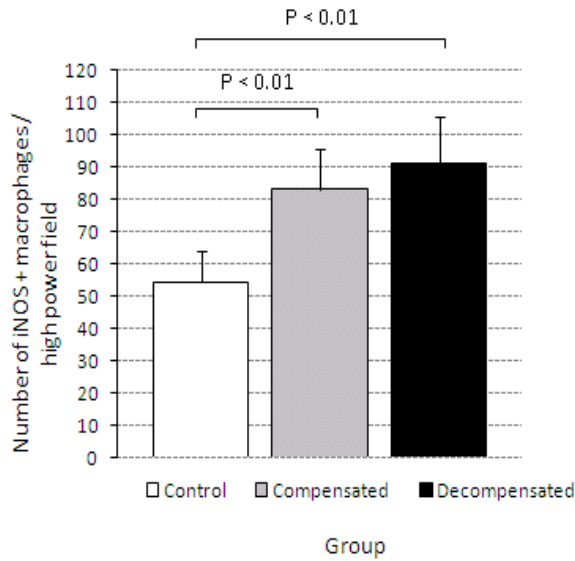
D


Figure 4. The presence in inducible nitric oxide synthase (iNOS) was assessed by IHC on paraffin-embedded tissue collected at endoscopy in controls, compensated and decompensated liver cirrhosis. Representative microphotographs are shown at low (x100) and high power (x400) magnification for controls (A), compensated cirrhosis (B) and decompensated cirrhosis (C). Significant increase in the number of iNOS positive macrophages was observed in compensated and decompensated cirrhosis compared to controls (D).

Gene expression after total RNA extraction from duodenal biopsies show increased expression of IL-8, CCL-2, CCL-13 and iNOS in patients with decompensated cirrhosis

A screening assay of 84 inflammatory genes by quantitative RT-PCR was performed to identify possible genes associated with decompensation. The following genes were found to be upregulated: TLR 1, 2, 6, IL-8, CCL-2, CCL-13 and iNOS (**Table 2**). Further quantitative analysis was performed using a customized qRT-PCR expression assay. In this assay, 27 genes including downstream pathways associated with TLR 4 activation, mitogen-activated protein kinase (MAPK) and NF kappa β ligand pathways as well as tight junction proteins were assessed. Final qRT-PCR analysis showed

significant upregulation at the mRNA level of four genes: IL-8, CCL-2, CCL-13 and iNOS in patients with decompensated cirrhosis. Of specific interest pathways signalling through NFκB were not upregulated.

Table 3 .Genes that were significantly up regulated in the Decompensated patient group

Gene symbol	Gene title	Fold regulation	p-value
CCL2	Chemokine (C-C motif) ligand 2	2.57	0.003*
CCL13	Chemokine (C-C motif) ligand 13	4.35	0.001*
IL8	Interleukin 8	2.84	0.027*
NOS2	Nitric oxide synthase 2, inducible	2.69	0.044*
*significant			

Increased Nitrite production in the duodenum of patients with decompensated cirrhosis

Total Nitrite reduction assay following Griess reaction was performed on the supernatant of short term biopsy cultures in decompensated (n=7), compensated (n=4) and control subjects (n=6). This analysis revealed a significant increase in the concentration of Total Nitrite when decompensated liver cirrhosis was compared to compensated liver cirrhosis and controls combined (p=0.04) (**figure 4A**).

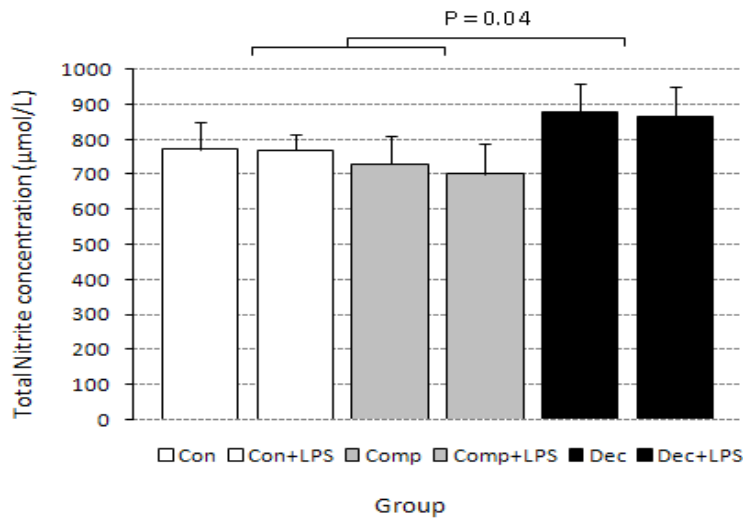
Elevated levels of CCL2/MCP-1, IL6 and IL8 are present in the culture supernatant of duodenum biopsies obtained from patients with decompensated liver disease

Expression of a number of cytokines was determined by means of cytometric bead array in the supernatant of short-term biopsy cultures. Similar to gene expression analysis IL6, CCL2/MCP-1 and IL8 (**figure 4B-D**) was found to be elevated in the supernatant of decompensated cirrhosis compared to controls.

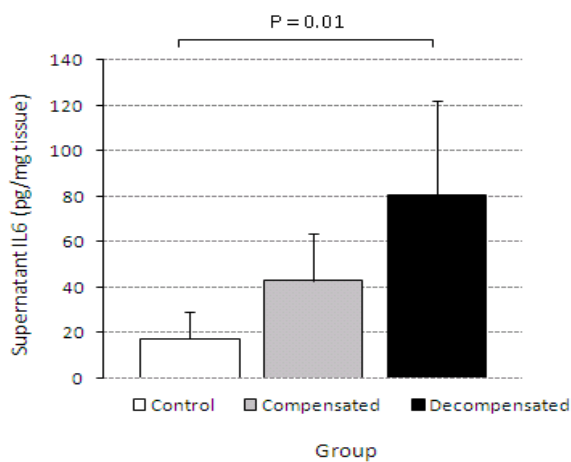
Enhanced levels of IL6 and IL8 were present in the serum of patients with Compensated and Decompensated cirrhosis

Corresponding to the local cytokine milieu in the duodenum, concentrations of IL6 and IL8 were also higher in the serum of patients with cirrhosis. There were also significant differences noticed between compensated and decompensated cirrhosis where these cytokines were expressed at higher levels in patients with advanced disease (**figure 5 E-F**).

A

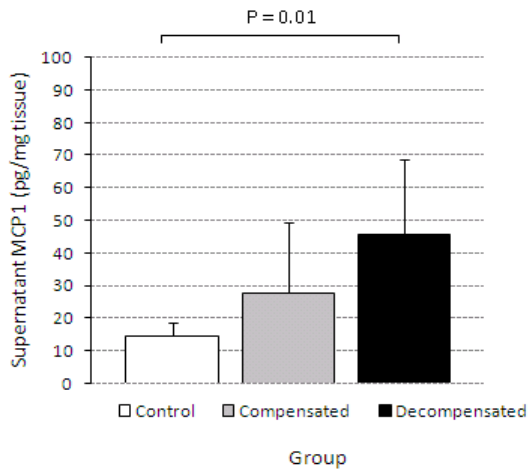


B

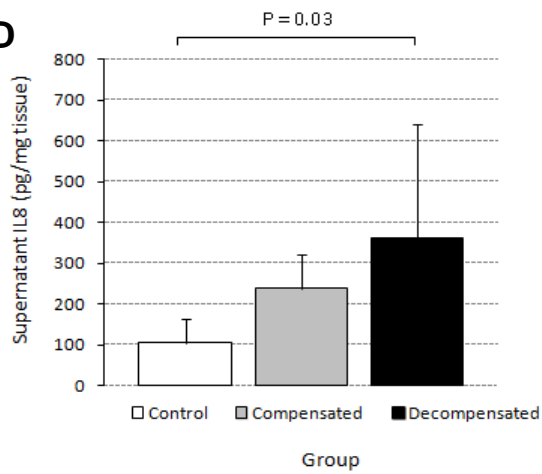


Chapter three: Results

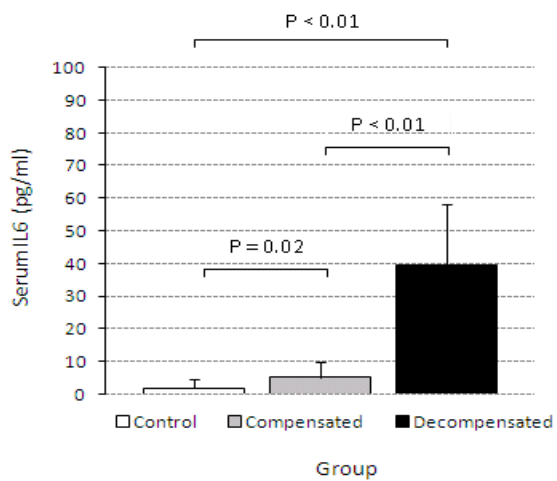
C



D



E



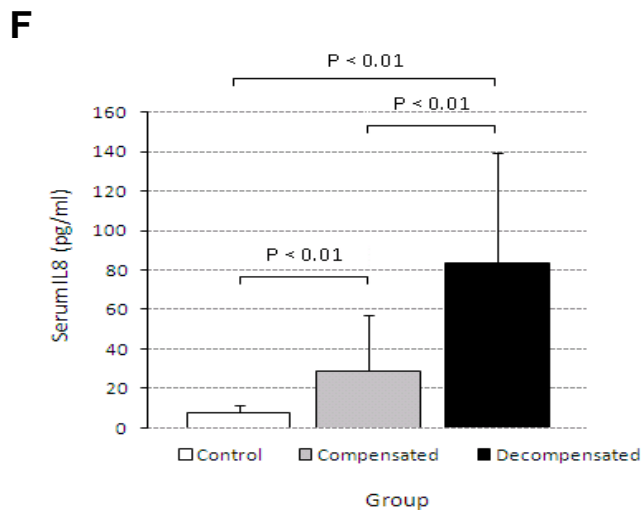


Figure 5. Increased NO levels were detected in the supernatant after 48 hours short term culture of duodenal biopsies in decompensated cirrhosis compared to NO duodenum in the compensated and control patients combined (A). Secretion of IL6 (B), CCL2/MCP-1 (C) and IL8 (D) were significantly enhanced in the supernatant of decompensated cirrhosis compared to controls. Corresponding to the gene expression findings and elevated cytokine levels in culture supernatant of decompensated cirrhosis is the increased levels of IL6 (E) and IL8 (F) in the plasma of these patients.

Pore forming tight junction protein, Claudin 2 is present at higher levels in decompensated cirrhosis compared to compensated cirrhosis and controls

There were no structural defects at the level of the epithelial barrier cells at the TEM level. Inter-epithelial junctions and junctional complexes assessed by TEM including desmosomes, tight, adherent and gap junctions appeared intact and no differences were observed between cirrhotics compared to controls (**figure 6A-B**). Representative tight junction proteins associated with structural integrity of the epithelial barrier including ZO, Occludins were not different at the mRNA and protein levels between controls and patients with cirrhosis. The pore forming protein Claudin-2 was not upregulated at the transcriptome level but significantly increased Claudin-2

protein levels were detected by Western blot in decompensated cirrhosis suggesting that Claudin-2 turnover is altered. There was no difference in the gap junction protein Connexion-43 associated with cell-to cell communication and repair between the groups (**figure 7A-E**).

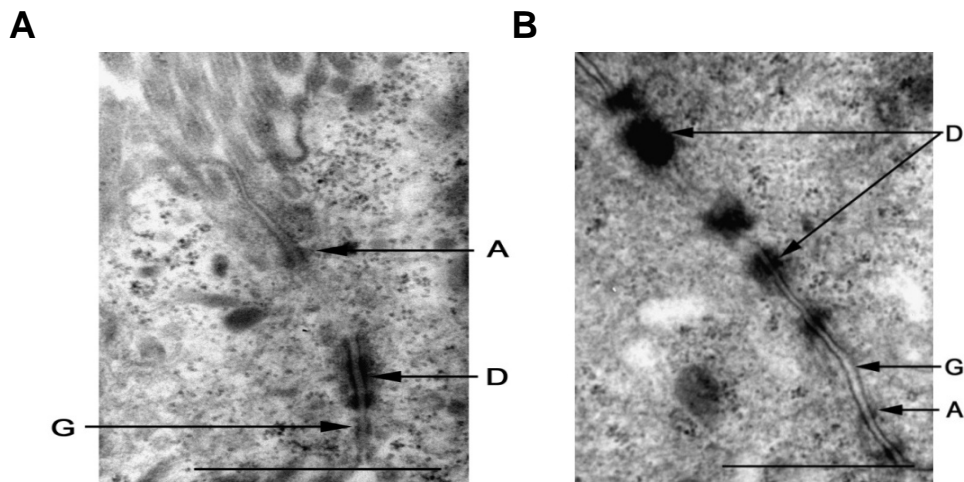


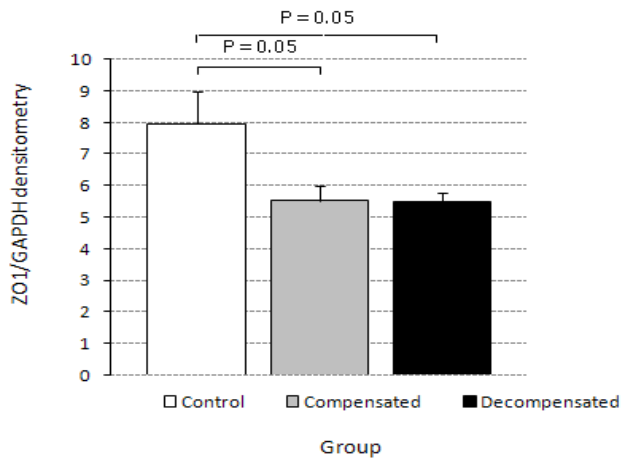
Figure 6.Electron microscopy showed intact epithelial barriers in both control (A) and decompensated (B) patients. Scale bars, 1μm. A = adherent junction D = desmosome G = gap junction

A

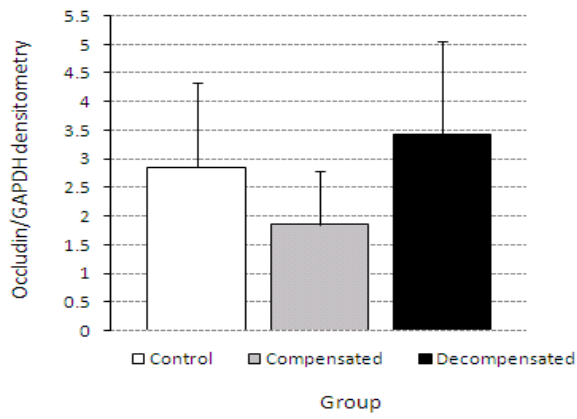
Protein	Protein size	Decompensated	Compensated	Control
ZO-1	226kDA			
Occludin	65 kDA			
Connexin 43 P[S368]	72 kDA			
Connexin 43	43 kDA			
Claudin 1	22 kDA			
Claudin 2	22 kDA			
GAPDH	37 kDA			

Chapter three: Results

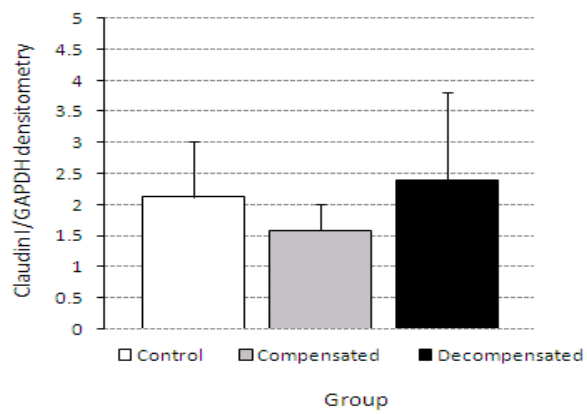
B



C



D



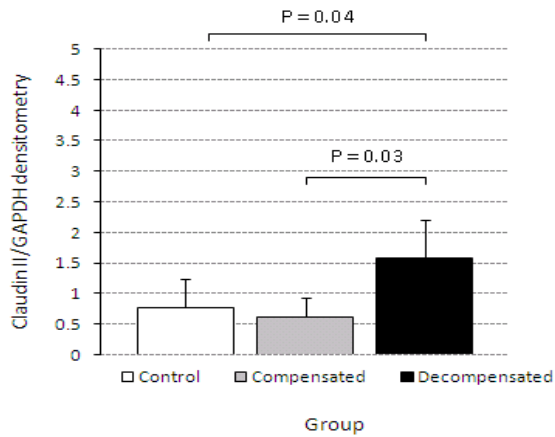
E


Figure 7. Western blot of tight junction proteins of two controls, two compensated and two decompensated patients. Claudin 2 was not detected in either control or compensated patients groups whereas it was present in decompensated liver cirrhosis (A). Densitometric evaluation of ZO-1 (B), Occludin (C), Claudin I (D) and Claudin II (E). ZO-1 was expressed slightly less in the compensated and decompensated patients than in controls while Claudin II protein was found to be significantly elevated in the decompensated patients than in the controls and compensated groups.

Chapter Four: Discussion

Bacterial infections are common in decompensated cirrhosis and have been associated with BT from the intestine. Even in the absence of viable organisms, the translocation of bactDNA and bacterial products can elicit an immune response associated with culture-positive infections²¹. Although factors such as altered bacterial flora, decreased intestinal motility and small bowel bacterial overgrowth²² have been associated with BT, the exact mechanism by which bacterial products cross the epithelial barrier remains poorly understood.

The intestinal epithelial barrier plays a central role in protecting the host from potentially harmful organisms. Not just by forming a specialized physical barrier, but also by maintaining intestinal immune homeostasis. Any structural changes or inability to maintain immune homeostasis will promote BT. Keeping this in mind we studied the mechanism of BT by assessing one of the most important host-defence cells of the innate immunity, the intestinal macrophage and possible inflammatory molecular pathways involved. As well as structural integrity of epithelial barrier with special focus on the integrity of tight junction proteins in patients with decompensated and compensated liver cirrhosis.

LPS, used as a surrogate for BT, were significantly elevated in the serum of patients with decompensated cirrhosis. A weak but significant correlation between Child-Pugh status and LPS levels were also detected. This finding is in keeping with previous studies that reported BT as a more frequent event in Child C than in Child A and Child B cirrhosis⁶.

Intestinal macrophages play a central role in regulation of the immune response against commensal bacteria¹⁸. In order to maintain mucosal homeostasis, intestinal macrophages typically do not express innate immune receptors such as CD14, CD16 and TREM-1¹⁶. Resident intestinal macrophages also do not produce pro-inflammatory cytokines, but still maintain the ability to effectively kill and phagocytose invading organisms^{17, 24}. On the contrary, certain diseases have been associated with activated intestinal macrophages. In IBD activated intestinal CD14⁺Trem-1⁺

macrophages¹⁸ respond to microbial stimulation and produce high levels of inflammatory cytokines^{25, 26}. Similarly, premature bacterial colonization of the intestinal mucosa of the preterm infant, before LPS tolerance has developed, leads to macrophage activation and mucosal inflammation resulting in necrotizing enterocolitis²⁷.

Flow-cytometric investigations showed that macrophages in the duodenum of decompensated cirrhosis display an activated phenotype expressing receptors for LPS (CD14) and Trem-1 at a significantly higher frequency than controls. The presence of these activated CD33+/CD14+ macrophages as to CD33+/CD14- intestinal macrophages that are typically found in the duodenum suggest that, either these activated macrophages are newly recruited blood monocytes or these cells are derived from a different subset of monocytes^{16, 18}.

Not only do these macrophages express innate receptors, but we were also able to show that they produce NO. iNOS expression in duodenal biopsies of decompensated cirrhosis was upregulated at mRNA and protein level. IHC revealed higher numbers of iNOS⁺ classically activated macrophages in the duodenum of both decompensated and compensated cirrhosis. Despite the increase in the numbers of activated macrophages, immunostaining showed that the total number of CD68⁺ macrophages did not differ in cirrhosis compared to controls. Furthermore, our study showed that macrophage activation is not caused by decompensation but rather preceded it since iNOS⁺ macrophages were detected in patients with compensated cirrhosis. This suggests that intestinal macrophage activation at the level of the gut wall is an early event in cirrhosis and may already reflect responses to altered bacterial flora and increased events of BT.

NO is one of the earliest acting, highly reactive and most potent pro-inflammatory molecules released by macrophages²⁸. A large body of evidence has accumulated indicating that NO plays an important role in BT. Pharmacological inhibition with a selective iNOS inhibitor, or genetic ablation of iNOS in knock-out animal models (iNOS^{-/-}) prevented LPS induced epithelial barrier dysfunction and bacterial translocation^{28, 29, 30}.

In addition to increased NOS2 levels, other inflammatory cytokines and chemokines (CCL-2, CCL-13 and IL-8) were also significantly upregulated at mRNA level. Elevated levels of CCL-2, IL-6 and IL-8 were detected in culture supernatant of decompensated cirrhosis while IL6 and IL8 were also increased in the serum of patients with cirrhosis. CCL-2 and CCL-13 are chemokines involved in the recruitment of monocytes³¹, while IL6 is a proinflammatory cytokine that is known to be upregulated in IBD (CD14+/TREM-1+ macrophages in Crohn's disease secrete IL6) and other sepsis syndromes³². It has recently been shown that IL-8, mostly known as a neutrophil chemotactant, released by intestinal epithelial cells and mononuclear cells in the lamina propria bind to ECM and serve as a potent chemotactic ligand for CD14+ blood monocytes³³. Previous studies showed that increased expression of IL-8 by endothelial cells can be induced by LPS³⁴ and IL-8 production is increased by exposure to E. coli in Crohn's disease³⁵. These findings suggest that elevated IL-8 observed in cirrhosis at the level of the duodenal wall and in the serum, is indeed in response to bacterial product translocation.

Interestingly, TNF levels were not different at the mRNA, culture or serum levels between the groups. In cirrhosis, in contrast to other inflammatory states, no activation of pathways associated with TLR4 mediated signalling (through MyD88, p38MAPK, TRAF, NFκB), necessary for the production of TNFα were observed. This suggests that increased iNOS expression is mediated by a TLR independent mechanism as has been observed in other conditions and is in keeping with the lack of severe inflammation and absence of ulceration observed at the level of the gut wall in cirrhosis compared to IBD or NEC.

The intestinal epithelium forms a barrier between the circulation and the external environment. This highly selective and regulated barrier permits ions, water and nutrients to be absorbed, but normally restricts the passage of harmful molecules, bacteria, viruses and other pathogens³⁶. In healthy individuals, the intestinal barrier is constituted of an intact layer of epithelial cells which are tightly connected by surrounding system of tight junction proteins³⁷. One of the functions of these TJ is to control paracellular permeability through the lateral intracellular space^{36, 38}. TJ consist of Zona-occludens, occludin and a large family of claudins³⁹. The exact

physiological role of these proteins, still needs to be determined but current consensus suggest that these proteins can be broadly separated into “barrier” and “pore” forming, with Claudin 2 being one of the best described “pore” forming TJ³⁹.

Tight junction dysregulation has been shown to be important in promoting BT. Recent studies have shown that increased intestinal permeability can be demonstrated in cirrhosis¹¹ and that decreased intestinal bile acids disrupt tight junctions⁴⁰. LPS when administered to wild type mice impaired gut barrier function by down regulating the expression of structural tight junction proteins²⁹, and induced bacterial translocation to mesenteric lymphnodes³⁰. In addition, activated macrophages in epithelial co-cultures inhibited enterocyte gap junctions through the effects of NO on connexin-43 mediated epithelial barrier communication and repair²⁸.

Ultra structural analysis by means of electron microscopy revealed an intact epithelial barrier in decompensated cirrhosis. This suggested that intestinal barrier permeability may be functionally changed by altered expression of tight junction proteins. We were not able to show any difference in the mRNA levels of ZO-1, occludin, claudin 1, 2 and connexin 43. Although protein analysis by means of western blot revealed a significant increase in the “pore” forming TJ claudin 2 in decompensated cirrhosis. Interestingly Claudin 2 expression was not increased in compensated liver disease nor was LPS, suggesting the importance of claudin 2 in increasing intestinal permeability to LPS during decompensation. Elevated Claudin-2 expression, associated with BT, has also been observed in other diseases such as Crohn's disease³⁸, Ulcerative Colitis³⁷ and Human immunodeficiency virus (HIV) infection⁴¹. Recently it was also demonstrated that IL-6 induced Claudin-2 expression in epithelial cell cultures and mouse intestine⁴².

Despite advances made in the understanding of altered bacterial flora and increased intestinal permeability in cirrhosis, the exact molecular mechanisms associated with bacterial translocation at the level of the gut are still unknown. In summary, our study showed the presence of activated CD14⁺Trem-1⁺iNOS⁺ intestinal macrophages, and increased levels of NO, IL-6 and claudin-2 levels in the duodenum of patients with decompensated

liver cirrhosis, suggesting that these factors enhance intestinal permeability to bacterial products. This is just the tip of the iceberg with regards to understanding BT in cirrhosis, future studies are needed such as the below mentioned to further understand BT and be able to develop possible treatment options :

- It is unknown whether the activated macrophage population seen in cirrhosis are able to effectively kill and phagocytose invading organisms, inability to efficiently remove bacteria will promote increased bacterial load to the liver
- Factors that drive monocytes to differentiate into CD33+/CD14-macrophages should be explored, it is possible that during a state of inflammation stromal factors responsible for macrophage differentiation are not released or are inactive.
- The physiological function of Claudin 2 needs to be explored. The mechanisms associated with claudin 2 expression, as well as the possibility that other structural proteins function in combination with claudin 2 to enhance barrier permeability.
- Isolated macrophages and epithelial cells, could be used to determine cytokines produced by specific cells as well as expression studies of alternative pathways associated with inflammation, could help determine the means by which these cytokines are produced.

Chapter Five: Summary

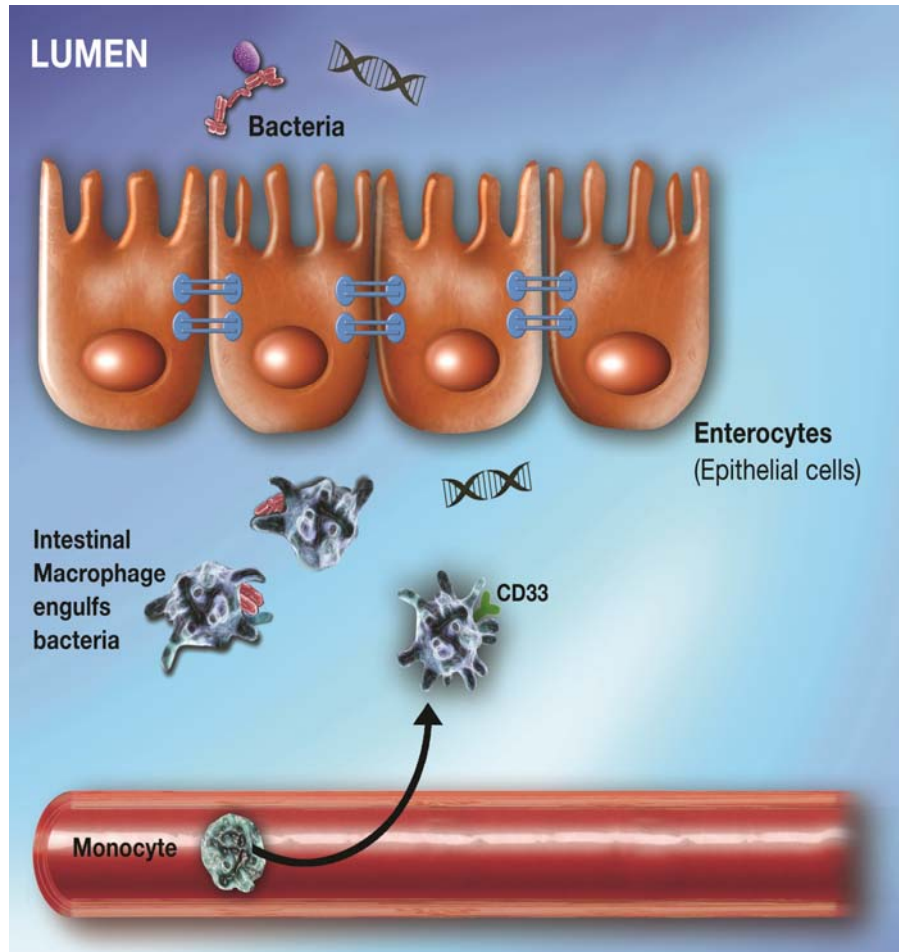


Figure 8. Intestinal macrophages in the normal intestine are very distinct in phenotype and function, although they are derived from blood monocytes, they do not express innate immune receptors such as CD14 and Trem-1, or produce inflammatory cytokines in response to bacterial products such as LPS but still maintain potent phagocytotic and bacteriocidal activity.

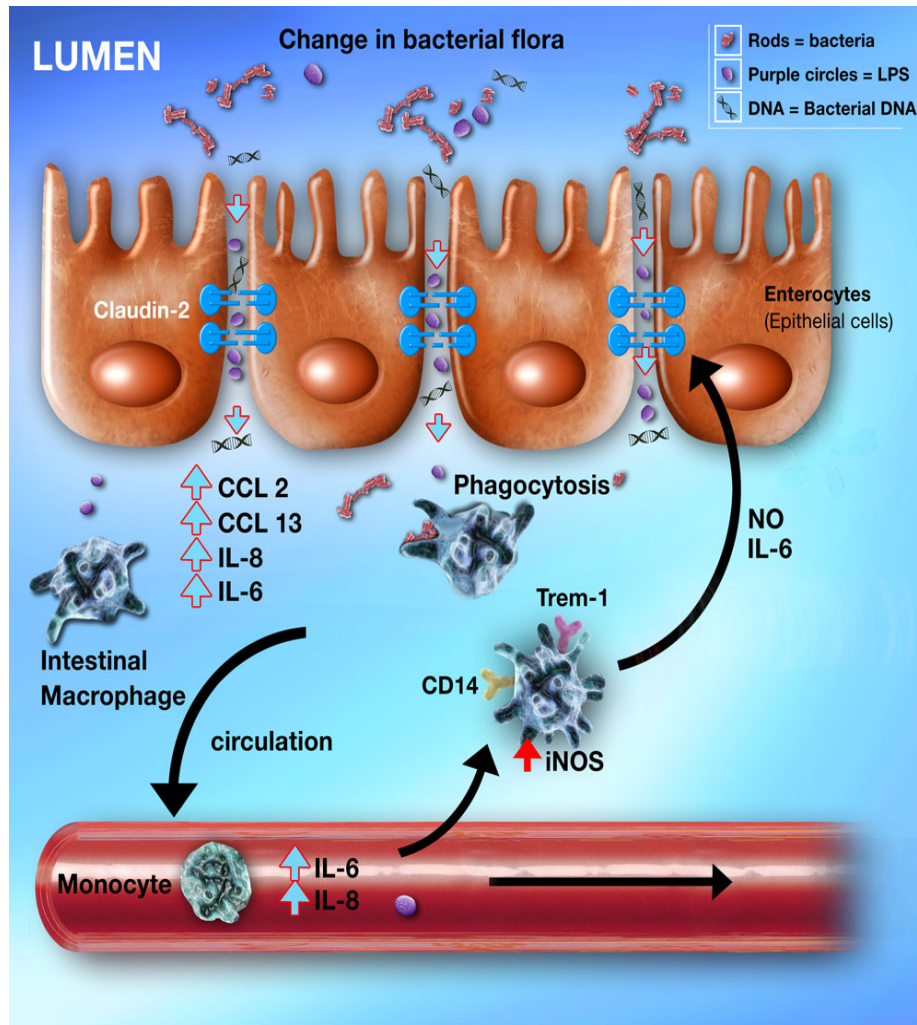


Figure 9. In the presence of altered bacterial flora and increased levels of chemokines activated $CD14^+$ / $Trem-1^+$ / $iNOS^+$ macrophages produce NO and IL-6 which increases Claudin-2 levels that in turn increases intestinal permeability and promote bacterial translocation.

References

1. Schuppan D, Afdhal NH. Liver cirrhosis. *Lancet* 2008;371:838-51
2. El-Naggar MM, Khalil EA, El-Daker MAM, *et al.* Bacterial DNA and its consequences in patients with cirrhosis and culture-negative, non-neutrocytic ascites. *Journal of Medical microbiology* 2008;57:1533-1538
3. Leber B, Mayrhauser U, Rybczynski M, *et al.* Innate immune dysfunction in acute and chronic liver disease. *Wien Klin Wochenschr* 2009;121:732-744
4. Neugebauer H, Hartmann P, Krenn S, *et al.* Bacterial translocation increases phagocytotic activity of polymorphonuclear leukocytes in portal hypertension: priming independent of liver cirrhosis. *Liver International* 2008;1478-3223
5. Riordan SM, Williams R. The intestinal flora and bacterial infection in cirrhosis. *Hepatology* 2006; 45:744-757.
6. Thalheimer U, Triantos CK, Samonakis DN, *et al.* Infection, coagulation, and variceal bleeding in cirrhosis. *Gut* 2005;54:556-563
7. Guarner C, Soriano G. Bacterial translocation and its consequences in patients with cirrhosis. *Eur J Gastroenterol Hepatol* 2005;17:27-31
8. Frances R, Zapater P, Gonzalez-Navajas JM, *et al.* Bacterial DNA in patients with cirrhosis and noninfected ascites mimics the soluble immune response established in patients with spontaneous bacterial peritonitis. *Hepatology* 2008;47:978-985
9. Zapater P, Frances R, Gonzalez-Navajas JM, *et al.* Serum and ascitic fluid bacterial DNA: A new independent prognostic factor in noninfected patients with cirrhosis. *Hepatology* 2008;48:1924-1931
10. Bellot P, García-Pagán JC, Francés R, *et al.* Bacterial DNA translocation is associated with systemic circulatory abnormalities and intrahepatic endothelial dysfunction in patients with cirrhosis. *Hepatology* 2010; 52:2044-52.
11. Scarpellini E, Valenza V, Gabrielli M, *et al.* Intestinal permeability in cirrhotic patients with and without spontaneous bacterial peritonitis: is the ring closed? *Am J Gastroenterol* 2010; 105:323-327

References

12. Son G, Kremer M, Hines IN. Contribution of GUT bacteria to liver pathobiology. *Gastroenterol Res Pract*. 2010; 2010:453563
13. Groschwitz KR, Hogan SP. Intestinal barrier function: Molecular regulation and disease pathogenesis. *J Allergy Clin Immunol* 2009;124:3-20
14. Weist R, Rath HC. Bacterial translocation in the gut. *Best Practise and Research Clinical Gastroenterology* 2003;17:397-425
15. Artis D. Epithelial-cell recognition of commensal bacteria and maintenance of immune homeostasis in the gut. *Nat Rev Immunol* 2008;8:411-420
16. Smith PD, Smythies LE, Greenwell-Wild T, *et al*. Intestinal macrophage response to microbial encroachment. *Mucosal Immunol*. 2011; 4:31-42.
17. Smythies LE, Sellers M, Clements RH, *et al*. Human intestinal macrophages display profound inflammatory anergy despite avid phagocytic and bacteriocidal activity. *J Clin Invest* 2005;115:66–75.
18. Schenk M, Bouchon A, Seibold F, *et al*. Trem-1 expressing intestinal macrophages crucially amplify chronic inflammation in experimental colitis and inflammatory bowel diseases. *J. Clin. Invest*. 2007;117:3097–310
19. Schneider T, Zippel T, Schmidt W, *et al*. Increased immunoglobulin G production by short term cultured duodenal biopsy samples from HIV infected patients. *Gut* 1998;42:357–361.
20. Moos V, Schmidt C, Geelhaar A, *et al*. Impaired Immune Functions of Monocytes and Macrophages in Whipple's Disease. *Gastroenterology* 2010;138:210–220
21. Guarner C, González-Navajas JM, Sánchez E, *et al*. The detection of bacterial DNA in blood of rats with CCl₄-induced cirrhosis with ascites represents episodes of bacterial translocation. *Hepatology*. 2006; 44:633-639.
22. Gunnarsdottir SA, Sadik R, Shev S, *et al*. Small Intestinal Motility Disturbances and Bacterial Overgrowth in Patients With Liver Cirrhosis and Portal Hypertension. *Am J Gastroenterol* 2003; 98:1362-1370
23. Kamada N, Hisamatsu T, Okamoto S, *et al*. Unique CD14+ intestinal macrophages contribute to the pathogenesis of Crohn disease via IL-23/INF- γ axis. *J Clin Invest* 2008;118:2269–2280.

References

24. Spottl T, Hausmann M, Kreutz M, *et al.* Monocyte differentiation in intestine-like macrophage phenotype induced by epithelial cells. *J Leukoc Biol* 2001;70:241-251
25. Smith AM, Rahman FZ, Hayee B, *et al.* Disordered macrophage cytokine secretion underlies impaired acute inflammation and bacterial clearance in Crohn's disease. *J Exp Med* 2009; 206:1883–1897.
26. Sheikh SZ, Matsuoka K, Kobayashi T, *et al.* Cutting Edge: IFN- γ is a negative regulator of IL-23 in murine macrophages and experimental colitis. *J Immunol* 2010; 184: 4069–4073.
27. Maheshwari A, Kelly DR, Nicola T, *et al.* TGF- β_2 suppresses macrophage cytokine production and mucosal inflammatory responses in the developing intestine. *Gastroenterology* 2011; 140:242-253.
28. Anand RJ, Dai S, Rippel C, *et al.* Activated macrophages inhibit enterocyte gap junctions via the release of nitric oxide. *Am J Physiol Gastrointest Liver Physiol* 2008;294:G109–G119.
29. Resta-Lenert S, Barrett KE. Enteroinvasive bacteria alter barrier and transport properties of human intestinal epithelium: Role of iNOS and COX-2. *Gastroenterology* 2002; 122:1070-1087.
30. Mishima S, Xu D, Lu Q, *et al.* Bacterial translocation is inhibited in inducible nitric oxide synthase knockout mice after endotoxin challenge but not in a model of bacterial overgrowth. *Arch Surg* 1997; 132:1190-1195.
31. Simpson KJ, Henderson NC, Bone-Larson CL, *et al.* Chemokines in the pathogenesis of liver disease: so many players with poorly defined roles. *Clinical Science* 2003; 104:47-63
32. Sanchez-Munoz F, Dominguez-Lopez A, Yamamoto-Furusho JK. Role of cytokines in inflammatory bowel disease. *World J Gastroenterol* 2008;14(27):4280-4288
33. Smythies LE, Maheshwari A, Clements R, *et al.* Mucosal IL8 and TGF-B recruit blood monocytes: evidence for cross-talk between the lamina propria stroma and myeloid cells. *J Leukoc Biol* 2006;80:492-499
34. Anand AR, Cucchiari M, Terwilliger EF, *et al.* The tyrosine kinase Pyk2 mediates lipopolysaccharide-induced IL-8 expression in human endothelial cells. *J Immunol* 2008; 180:5636-5644.

References

35. Martin HM, Campbell BJ, Hart CA, *et al.* Enhanced Escherichia coli adherence and invasion in Crohn's disease and colon cancer. *Gastroenterology* 2004;127:80–93.
36. John LJ, Fromm M, Schulzke JD. Epithelial Barriers in Intestinal Inflammation. *Antioxid Redox Signal* 2011 May 11. [Epub ahead of print]
37. Zeissig S, Bürgel N, Günzel D, *et al.* Changes in expression and distribution of claudin 2, 5 and 8 lead to discontinuous tight junctions and barrier dysfunction in active Crohn's disease. *Gut* 2007; 56:61-72.
38. Han X, Fink MP, Yang R, *et al.* Increased iNOS activity is essential for intestinal epithelial tight junction dysfunction in endotoxemic mice. *Shock* 2004; 21:261-270
39. Shen L, Weber CR, Raleigh DR, *et al.* Tight junction pore and leak pathways: a dynamic duo. *Annu Rev Physiol* 2011;73:283-309
40. Yang R, Harada T, Li J, *et al.* Bile modulates intestinal epithelial barrier function via an extracellular signal related kinase 1/2 dependent mechanism. *Intensive Care Med* 2005; 31:709-17
41. Smith AJ, Schacker TW, Reilly CS, *et al.* A role for syndecan-1 and claudin-2 in microbial translocation during HIV-1 infection. *J Acquir Immune Defic Syndr* 2010;1;55:306-315
42. Suzuki T, Yoshinaga N, Tanabe S. IL6 regulates claudin-2 expression and tight junction permeability in intestinal epithelium. *J Biol Chem* 2011 Jul 19. [Epub ahead of print]

Appendices

Appendix A:

Graphs and histograms of cell populations selected and studied by means of flow cytometry

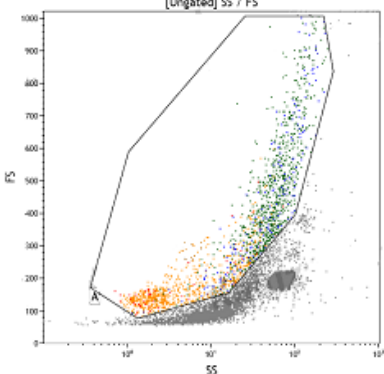
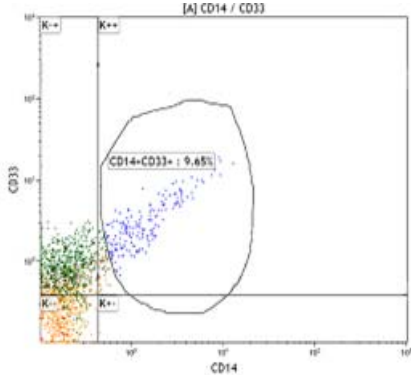
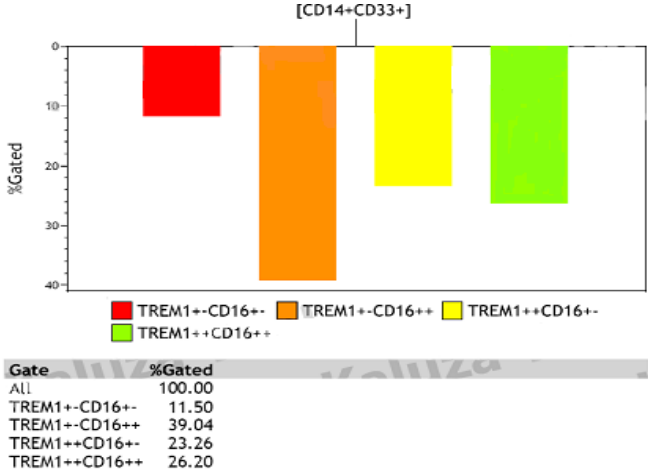
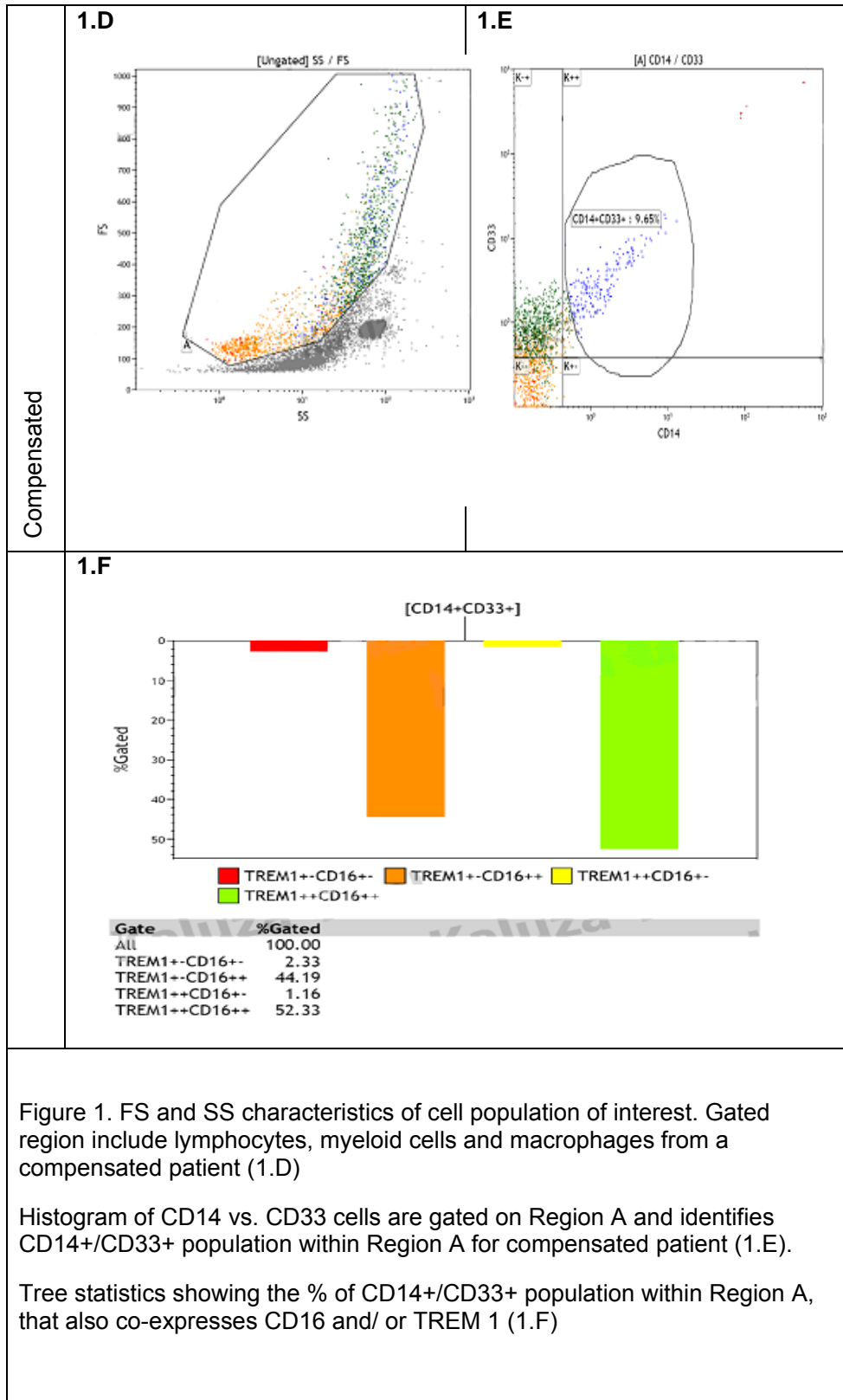
	Forward scatter (FS) and Side scatter (SS) characteristics	Histogram of CD33+/CD14+ populations											
Control	<p>1.A</p> 	<p>1.B</p> 											
	<p>1.C</p>  <table border="1"> <thead> <tr> <th>Gate</th> <th>%Gated</th> </tr> </thead> <tbody> <tr> <td>All</td> <td>100.00</td> </tr> <tr> <td>TREM1+-CD16-+</td> <td>11.50</td> </tr> <tr> <td>TREM1+-CD16++</td> <td>39.04</td> </tr> <tr> <td>TREM1++CD16-+</td> <td>23.26</td> </tr> <tr> <td>TREM1++CD16++</td> <td>26.20</td> </tr> </tbody> </table>	Gate	%Gated	All	100.00	TREM1+-CD16-+	11.50	TREM1+-CD16++	39.04	TREM1++CD16-+	23.26	TREM1++CD16++	26.20
Gate	%Gated												
All	100.00												
TREM1+-CD16-+	11.50												
TREM1+-CD16++	39.04												
TREM1++CD16-+	23.26												
TREM1++CD16++	26.20												

Figure 1. FS and SS characteristics of cell population of interest. Gated region include lymphocytes, myeloid cells and macrophages from a control patient (1.A)

Histogram of CD14 vs. CD33 cells are gated on Region A and identifies CD14+/CD33+ population within Region A for control (1.B).

Tree statistics showing the % of CD14+/CD33+ population within Region A, that also co-expresses CD16 and/ or TREM 1 (1.C)

Appendices



Appendices

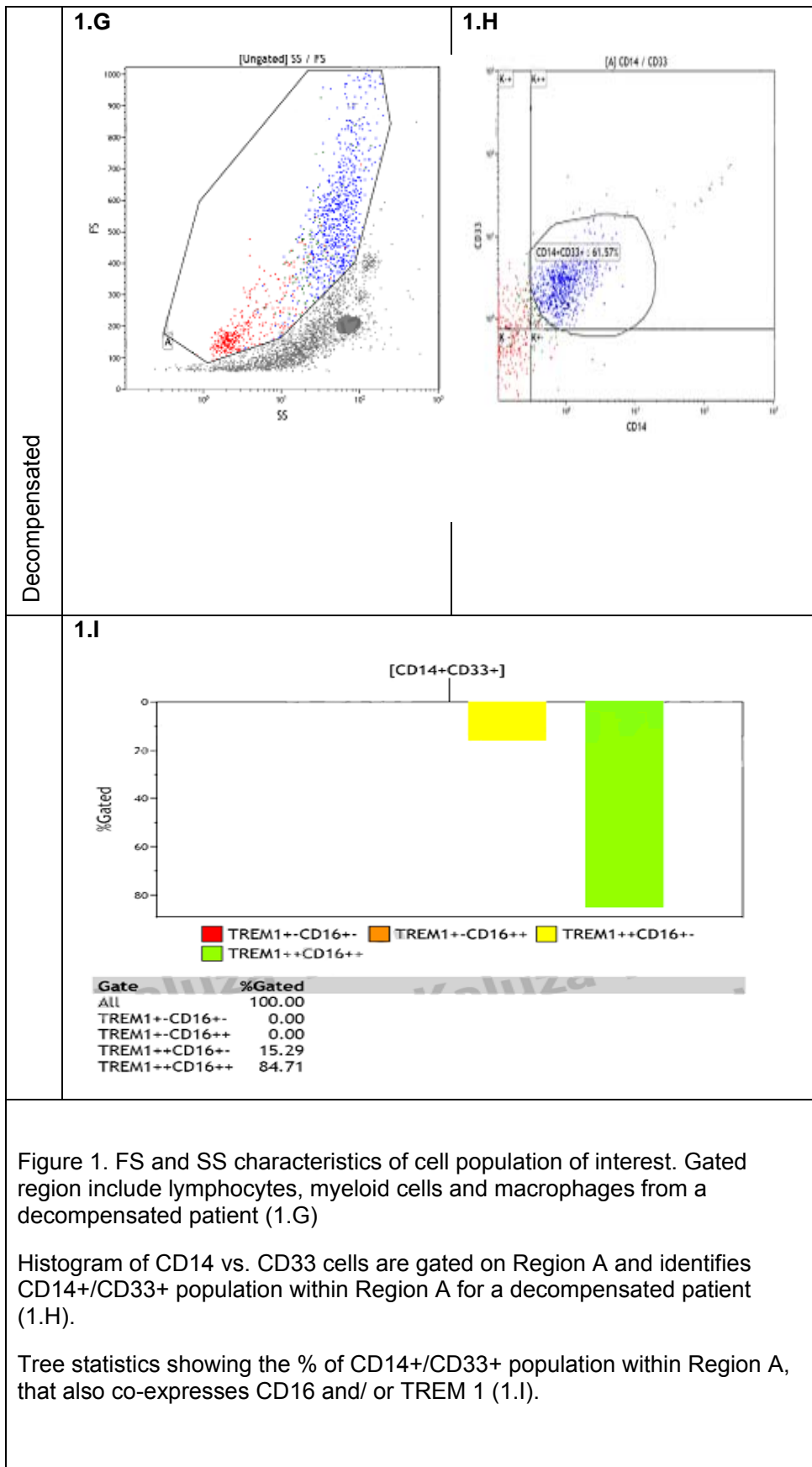


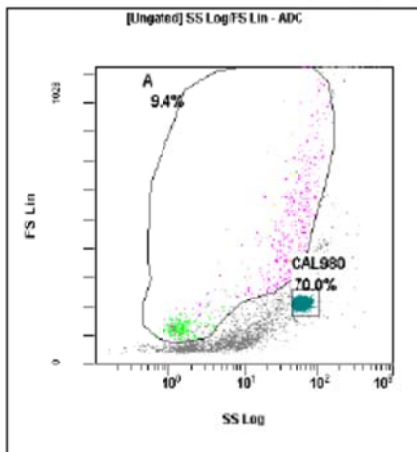
Figure 1. FS and SS characteristics of cell population of interest. Gated region include lymphocytes, myeloid cells and macrophages from a decompensated patient (1.G)

Histogram of CD14 vs. CD33 cells are gated on Region A and identifies CD14+/CD33+ population within Region A for a decompensated patient (1.H).

Tree statistics showing the % of CD14+/CD33+ population within Region A, that also co-expresses CD16 and/ or TREM 1 (1.I).

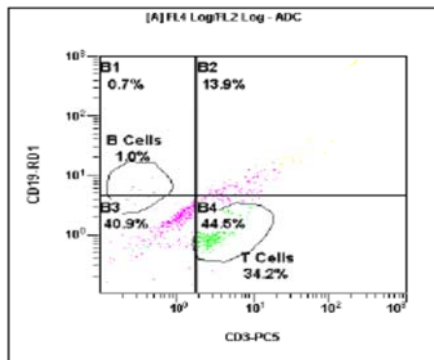
Appendices

1. J



[Ungated] SS Log/FS Lin					
Region	Number	%Total	%Gated	X-Mean	Y-Mean
ALL	9493	100.00	100.00	50.7	214
A	890	9.38	9.38	31.3	346
CAL	6648	70.03	70.03	60.4	214

1. K



[A] FL4 Log/FL2 Log					
Region	Number	%Total	%Gated	X-Mean	Y-Mean
ALL	890	9.38	100.00	5.74	9.85
B Cells	9	0.09	1.01	0.323	5.49
B1	6	0.06	0.67	0.329	6.32
B2	124	1.31	13.93	27	59.5
B3	364	3.83	40.90	1.08	1.82
B4	396	4.17	44.49	3.47	1.74
T Cells	304	3.20	34.16	3.55	1.15

Figure 1.FS vs. SS Histogram of a Decompensated biopsy sample. Gated region A identifies population of interest, including lymphocytes, myeloid cells and macrophages (1.J)

CD19 vs. CD3 Histogram, gated on Region A, identifies the B and T cell populations within the biopsy of a decompensated patient (1.K).

Appendices

Appendix B:

Nanodrop and Experion readings confirming RNA quantity and quality

Table 1. Only samples with a concentration of > 250ng/ul as well as 260/280 and 260/230 ratio's > 2 were used for cDNA synthesis.

Sample ID	User ID	Date	Time	ng/ul	A260	A280	260/280	260/230	Constant	Cursor Pos.	Cursor abs.	340 raw
H2O	Default	2010/12/15	02:26 PM	-0.52	-0.013	-0.027	0.48	0.75	40.00	230	-0.017	0.007
PHTG65(1)	Default	2010/12/15	02:27 PM	529.12	13.228	6.428	2.06	2.12	40.00	230	6.230	0.178
PHTG65(2)	Default	2010/12/15	02:28 PM	533.87	13.347	6.469	2.06	2.11	40.00	230	6.316	0.097
H2O	Default	2010/12/15	02:29 PM	2.82	0.071	0.027	2.64	2.63	40.00	230	0.327	0.067
H2O (2)	Default	2010/12/15	02:30 PM	0.16	0.004	-0.001	-4.84	-0.11	40.00	230	-0.036	0.013
PHTG72(1)	Default	2010/12/15	02:31 PM	372.44	9.311	4.552	2.05	2.06	40.00	230	4.524	0.259
PHTG72(2)	Default	2010/12/15	02:31 PM	376.61	9.415	4.604	2.04	2.07	40.00	230	4.540	0.216
H2O	Default	2010/12/15	02:32 PM	-0.16	-0.004	-0.022	0.18	0.14	40.00	230	-0.029	0.003
PHTG78(1)	Default	2010/12/15	02:33 PM	305.24	7.631	3.690	2.07	2.13	40.00	230	3.589	0.096
PHTG78(2)	Default	2010/12/15	02:34 PM	313.51	7.838	3.808	2.06	2.14	40.00	230	3.569	0.088
H2O	Default	2010/12/15	02:35 PM	0.13	0.003	-0.005	-0.67	-0.13	40.00	230	-0.025	-0.013
PHTG79(1)	Default	2010/12/15	02:35 PM	420.76	10.519	5.173	2.03	2.13	40.00	230	4.328	0.141
PHTG79(2)	Default	2010/12/15	02:36 PM	426.88	10.672	5.266	2.03	2.13	40.00	230	5.313	0.148
H2O	Default	2010/12/15	02:37 PM	1.97	0.049	0.004	13.78	2.33	40.00	230	0.321	0.003

Well ID	Sample Name	RQI
1	PHTG A	9
2	PHTG B	9
3	PHTG D	9.2
4	PHTG F	8.4
5	PHTG G	8.5
6	PH 1	8.1
7	PH 2	8.8
8	PH 3	9.2
9	PHTG 006	9.9
10	PHTG 010	9.7
11	PHTG 015	9.1
12	PHTG 029	9.6

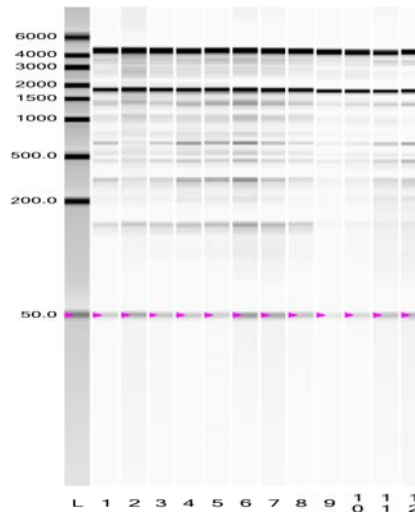


Figure 2. Experion analysis. Only samples with a RQI value > 7 and that showed minimal degradation was used for further gene expression analysis

Appendix C:

Examples of amplification and Melt curves generation during gene expression analysis

Amplification curves

Melt curves

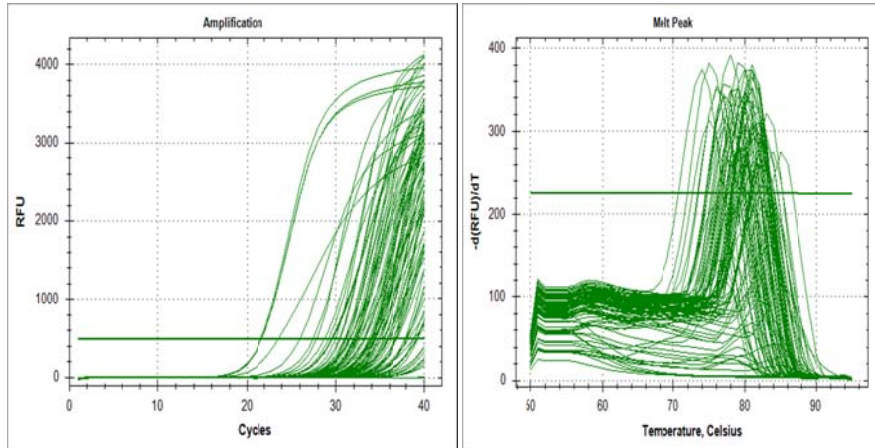


Figure 3. Example of amplification and melt curves generated during gene expression analysis

Appendix D:

Genes included in the Human Inflammatory response and Autoimmunity (PAHS-077A) RT² Profiler™ Array

Gene symbol	GeneBank	Official full name
BCL6	NM_001706	B-cell CLL/lymphoma 6
C3	NM_000064	Complement component 3
C3AR1	NM_004054	Complement component 3a receptor 1
C4A	NM_007293	Complement component 4A (Rodgers blood group)
CCL11	NM_002986	Chemokine (C-C motif) ligand 11
CCL13	NM_005408	Chemokine (C-C motif) ligand 13
CCL16	NM_004590	Chemokine (C-C motif) ligand 16
CCL17	NM_002987	Chemokine (C-C motif) ligand 17
CCL19	NM_006274	Chemokine (C-C motif) ligand 19
CCL2	NM_002982	Chemokine (C-C motif) ligand 2
CCL21	NM_002989	Chemokine (C-C motif) ligand 21
CCL22	NM_002990	Chemokine (C-C motif) ligand 22
CCL23	NM_005064	Chemokine (C-C motif) ligand 23
CCL24	NM_002991	Chemokine (C-C motif) ligand 24
CCL3	NM_002983	Chemokine (C-C motif) ligand 3
CCL4	NM_002984	Chemokine (C-C motif) ligand 4
CCL5	NM_002985	Chemokine (C-C motif) ligand 5
CCL7	NM_006273	Chemokine (C-C motif) ligand 7
CCL8	NM_005623	Chemokine (C-C motif) ligand 8
CCR1	NM_001295	Chemokine (C-C motif) receptor 1
CCR2	NM_001123 396	Chemokine (C-C motif) receptor 2
CCR3	NM_001837	Chemokine (C-C motif) receptor 3
CCR4	NM_005508	Chemokine (C-C motif) receptor 4
CCR7	NM_001838	Chemokine (C-C motif) receptor 7

Appendices

CD40	NM_001250	CD40 molecule, TNF receptor superfamily member 5
CD40LG	NM_000074	CD40 ligand
CEBPB	NM_005194	CCAAT/enhancer binding protein (C/EBP), beta
CRP	NM_000567	C-reactive protein, pentraxin-related
CSF1	NM_000757	Colony stimulating factor 1 (macrophage)
CXCL1	NM_001511	Chemokine (C-X-C motif) ligand 1 (melanoma growth stimulating activity, α)
CXCL10	NM_001565	Chemokine (C-X-C motif) ligand 10
CXCL2	NM_002089	Chemokine (C-X-C motif) ligand 2
CXCL3	NM_002090	Chemokine (C-X-C motif) ligand 3
CXCL5	NM_002994	Chemokine (C-X-C motif) ligand 5
CXCL6	NM_002993	Chemokine (C-X-C motif) ligand 6 (granulocyte chemotactic protein 2)
CXCL9	NM_002416	Chemokine (C-X-C motif) ligand 9
CXCR4	NM_003467	Chemokine (C-X-C motif) receptor 4
FASLG	NM_000639	Fas ligand (TNF superfamily, member 6)
FLT3LG	NM_001459	Fms-related tyrosine kinase 3 ligand
FOS	NM_005252	FBJ murine osteosarcoma viral oncogene homolog
HDAC4	NM_006037	Histone deacetylase 4
IFNG	NM_000619	Interferon, gamma
IL10	NM_000572	Interleukin 10
IL10RB	NM_000628	Interleukin 10 receptor, beta
IL18	NM_001562	Interleukin 18 (interferon-gamma-inducing factor)
IL18RAP	NM_003853	Interleukin 18 receptor accessory protein
IL1A	NM_000575	Interleukin 1, alpha
IL1B	NM_000576	Interleukin 1, beta
IL1F10	NM_173161	Interleukin 1 family, member 10 (theta)
IL1R1	NM_000877	Interleukin 1 receptor, type I
IL1RAP	NM_002182	Interleukin 1 receptor accessory protein
IL1RN	NM_000577	Interleukin 1 receptor antagonist

Appendices

IL22	NM_020525	Interleukin 22
IL22RA2	NM_052962	Interleukin 22 receptor, alpha 2
IL23A	NM_016584	Interleukin 23, alpha subunit p19
IL23R	NM_144701	Interleukin 23 receptor
IL6	NM_000600	Interleukin 6 (interferon, beta 2)
IL6R	NM_000565	Interleukin 6 receptor
IL8	NM_000584	Interleukin 8
CXCR1	NM_000634	Chemokine (C-X-C motif) receptor 1
CXCR2	NM_001557	Chemokine (C-X-C motif) receptor 2
IL9	NM_000590	Interleukin 9
ITGB2	NM_000211	Integrin, beta 2 (complement component 3 receptor 3 and 4 subunit)
KNG1	NM_000893	Kininogen 1
LTA	NM_000595	Lymphotoxin alpha (TNF superfamily, member 1)
LTB	NM_002341	Lymphotoxin beta (TNF superfamily, member 3)
LY96	NM_015364	Lymphocyte antigen 96
MYD88	NM_002468	Myeloid differentiation primary response gene (88)
NFATC3	NM_004555	Nuclear factor of activated T-cells, cytoplasmic, calcineurin-dependent 3
NFKB1	NM_003998	Nuclear factor of kappa light polypeptide gene enhancer in B-cells 1
NOS2	NM_000625	Nitric oxide synthase 2, inducible
NR3C1	NM_000176	Nuclear receptor subfamily 3, group C, member 1 (glucocorticoid receptor)
RIPK2	NM_003821	Receptor-interacting serine-threonine kinase 2
TIRAP	NM_001039 661	Toll-interleukin 1 receptor (TIR) domain containing adaptor protein
TLR1	NM_003263	Toll-like receptor 1
TLR2	NM_003264	Toll-like receptor 2
TLR3	NM_003265	Toll-like receptor 3
TLR4	NM_138554	Toll-like receptor 4
TLR5	NM_003268	Toll-like receptor 5

Appendices

TLR6	NM_006068	Toll-like receptor 6
TLR7	NM_016562	Toll-like receptor 7
TNF	NM_000594	Tumor necrosis factor
TNFSF14	NM_003807	Tumor necrosis factor (ligand) superfamily, member 14
TOLLIP	NM_019009	Toll interacting protein
B2M	NM_004048	Beta-2-microglobulin
HPRT1	NM_000194	Hypoxanthine phosphoribosyltransferase 1
RPL13A	NM_012423	Ribosomal protein L13a
GAPDH	NM_002046	Glyceraldehyde-3-phosphate dehydrogenase
ACTB	NM_001101	Actin, beta

Appendix E:

Genes included in CAPH09859D customized RT² Profiler PCR array

Gene Symbol	GeneBank	Official Full Name
TLR1	NM_003263	toll-like receptor 1
TLR2	NM_003264	toll-like receptor 2
TLR4	NM_138554	toll-like receptor 4
TLR6	NM_006068	toll-like receptor 6
NOD1	NM_006092	nucleotide-binding oligomerization domain containing 1
NOD2	NM_022162	nucleotide-binding oligomerization domain containing 2
TLR9	NM_017442	toll-like receptor 9
TIRAP	NM_001039661	toll-interleukin 1 receptor (TIR) domain containing adaptor protein
TRAF6	NM_004620	TNF receptor-associated factor 6
MAPK14	NM_001315	mitogen-activated protein kinase 14
MAPK1	NM_002745	mitogen-activated protein kinase 1
MAPK8	NM_002750	mitogen-activated protein kinase 8
JUN	NM_002228	jun oncogene
NFKB1	NM_003998	nuclear factor of kappa light polypeptide gene enhancer in B-cells 1
CEBPB	NM_005194	CCAAT/enhancer binding protein (C/EBP), beta
GJA1	NM_000165	gap junction protein, alpha 1
TJP1	NM_175610	tight junction protein 1 (zona occludens 1)
CLDN1	NM_021101	claudin 1
CLDN2	NM_020384	claudin 2
OCLN	NM_002538	occludin
NOS2	NM_000625	nitric oxide synthase 2, inducible

Appendices

CCL2	NM_002982	chemokine (C-C motif) ligand 2
CCL13	NM_005408	chemokine (C-C motif) ligand 13
IL8	NM_000584	interleukin 8
IL22	NM_020525	interleukin 22
il10	NM_000572	interleukin 10
TGFB1	NM_000660	Transforming growth factor, beta 1
RPL13A	NM_012423	ribosomal protein L13a
B2M	NM_004048	beta-2-microglobulin
HGDC	SA_00105	Human Genomic DNA Contamination
RTC	SA_00104	Reverse Transcription Control
PPC	SA_00103	Positive PCR Control

Declaration:

I, Johannie du Plessis hereby declare that this dissertation is my own work and has not been presented by me for any degree at this or any other University:

Signed:

Date:

Department of Immunology, School of Health Sciences, University of Pretoria,
South Africa

Acknowledgements:

Prof. Schalk W van der Merwe

I am grateful for given the opportunity to be part of this project. Thank you for your encouragement, guidance and support from the initial to final level enabling me to develop an understanding of the subject. Thank you for keeping me focused on the important issues, having faith in my work and for always being a strong advocate for me. You helped me develop a deep passion for science. I am looking forward to working with you for the next few years.

Dr Tomas Slavik, Melony Jordaan, Voula Stivaktas, Dr Mervyn Beukes, Stefan van Wyk, Prof Resia Pretorius, Warren Vieira, Dr Helen Steel and Prof Ronnie Anderson

Thank you for contributing your expertise and valuable time to the realization of this research. It is obvious that any success I may have achieved is at least partially dependent on your inputs. This project would not have been possible without you.

Dr Martin Nieuwoudt

I am grateful for your guidance with regards to the statistical analysis detailed review, constructive criticism and excellent advice during the preparation of this dissertation.

Leonie Roos

Thank you for being part of this project, for sharing excitement, frustration and lots of tea with me. The months we worked together have been the most enjoyable I have experienced.

Dr Johan van Beljon, Dr Apostel Pappas, Prof Hennie Becker, Dr Fritz Potgieter, Dr Jochum Terhaar and the staff of GI-unit Pretoria East Hospital as well as the staff of GI-unit Steve Biko Academic Hospital.

Thank you for your help and interest in our projects. Your participation has been critical to our success.

My parents, Andries and Cornelia du Plessis and Grandmother Joey Ollewagen.

Thank you for granting the opportunity to continue postgraduate studies, it would not have been possible without your emotional and financial support.

Adriaan van Wyk

Thank you for your patience and encouragement. This dissertation is dedicated to you



* **FWA** 00002567, Approved dd 22 May 2002 and Expires 24 Jan 2009.

* **IRB** 0000 2235 IORG0001762 Approved dd Jan 2006 and Expires 13 Aug 2011.

Date: 30/10/2008

PROTOCOL NO.	152/2008
PROTOCOL TITLE	Assessing the role of infection in cirrhotic and non-cirrhotic portal hypertensive patients presenting with variceal bleeding.
INVESTIGATOR	Principle Investigator: Professor S W van der Merwe svdmerwel@mweb.co.za
DEPARTMENT	Dept: Gastroenterology and Hepatology Research Unit Phone: 012-3192352 Fax: 012-3283600 E-Mail: johannie_duplessis@hotmail.com
STUDY DEGREE	None
SPONSOR	None
MEETING DATE OF THIS STUDY	27/08/2008

This **Protocol** and **Informed Consent** have been considered by the Faculty of Health Sciences Research Ethics Committee, University of Pretoria on 22/10/2008 and found to be acceptable

* *Members attended & Feedback at the meeting .*

- *Dr A Nienaber (female) BA (Hons) (Wits); LLB; LLM (UP); Dipl.Datametrics (UNISA)
- *Prof V.O.L. Karusseit MBChB; MFGP (SA); MMed (Chir); FCS (SA)
- *Prof M Kruger (female) MB.ChB. (Pta); MMed. Pead. (Pret); PhD. (Leuven)
- *Dr N K Likibi MB.BCh; Med.Adviser (Gauteng Dept.of Health)
- *Dr T S Marcus (female) BSc (LSE), PhD (University of Lodz, Poland)
- *Mrs M C Nzeku (female) BSc (NUL); MSc Biochem (UCL, UK)
- *Snr Sr J. Phatoli (female) BCur (Eet.A) BTec (Oncology Nursing Science) Snr Nursing-Sister
- *Dr L Schoeman (female) BP harm, BA Hons (PSy), PhD
- *Dr R Sommers (female) MBChB; MMed (Int); MPharMed;
- *Mr Y Sikweyiya MPH; Master Level Fellowship in Research Ethics; BSC (Health Promotion)
Postgraduate Dip in Health Promotion
- *Prof TJP Swart BChD, MSc (Odont), MChD (Oral Path), PGCHE
- *Dr A P van Der Walt BChD, DGA (Pret) Director: Clinical Services of the Pretoria Academic Hospital
- *Prof C W van Staden MBChB; MMed (Psych); MD; FCPsych; FTCL; UPLM; Dept of Psychiatry

Dr R Sommers; MBChB; MMed (Int); MPharMed.

SECRETARIAT of the Faculty of Health Sciences Research Ethics Committee, University of Pretoria, Pretoria Academic Hospital

◆ H W Snyman Building (South) Level 2-34 ◆ P.O.BOX 667 Pretoria, South Africa, 0001 ◆ Tel:(012)3541330 ◆
◆ Fax: (012)3541367 / 0866515924 ◆ E-Mail: manda@med.up.ac.za ◆ Web: [//www.healthethics-up.co.za](http://www.healthethics-up.co.za) ◆